Available online at www.sciencedirect.com
ScienceDirect
Geochimica et Cosmochimica Acta 72 (2008) 3907–3927
Geochimica et Cosmochimica Acta
www.elsevier.com/locate/gca

Seasonal $\delta^{34}S$ variations in two high elevation snow pits measured by ^{33}S–^{36}S double spike thermal ionization mass spectrometry

Jacqueline L. Mann [a,b,*], Christopher A. Shuman [c], W. Robert Kelly [a], Karl J. Kreutz [d]

[a] *National Institute of Standards and Technology, Analytical Chemistry Division, Chemical Science and Technology Laboratory, Inorganic Chemical Metrology Group, 100 Bureau Drive, MS 8391, Gaithersburg, MD 20899-8391, USA*
[b] *University of Maryland, Department of Geology, College Park, MD 20742, USA*
[c] *University of Maryland, Baltimore County, Goddard Earth Science and Technology Center, NASA Goddard Space Flight Center, Code 698, Greenbelt, MD 20771, USA*
[d] *Climate Change Institute and Department of Earth Sciences, 236 Sawyer Hall, University of Maine, Orono, ME 04469, USA*

Received 10 January 2008; accepted in revised form 18 May 2008; available online 28 May 2008

Abstract

$\delta^{34}S$ and sulfate concentrations were determined in snow pit samples using a thermal ionization mass spectrometric technique capable of 0.2‰ accuracy and requires ≈5 μg (0.16 μmol) natural S. The technique utilizes a ^{33}S–^{36}S double spike for instrumental mass fractionation correction, and has been applied to snow pit samples collected from the Inilchek Glacier, Kyrgyzstan and from Summit, Greenland. These $\delta^{34}S$ determinations provide the first high-resolution seasonal data for these sites, and are used to estimate seasonal sulfate sources. Deuterium (δD) and oxygen ($\delta^{18}O$) isotope data show that the Inilchek and Summit snow pit samples represent precipitation over ≈20 months.

The $\delta^{34}S$ values for the Inilchek ranged from +2.6 ± 0.4‰ to +7.6 ± 0.4‰ on sample sizes ranging from 0.3 to 1.8 μmol S. $\delta^{34}S$ values for Greenland ranged from +3.6 ± 0.7‰ to +13.3 ± 5‰ for sample sizes ranging from 0.05 to 0.29 μmol S. The SO_4^{2-} concentration ranged from 92.6 ± 0.4 to 1049 ± 4 ng/g for the Inilchek and 18 ± 9 to 93 ± 6 ng/g for the Greenland snow pit. Anthropogenic sulfate dominates throughout the sampled time interval for both sites based on mass balance considerations. Additionally, both sites exhibit a seasonal signature in both $\delta^{34}S$ and SO_4^{2-} concentration. The thermal ionization mass spectrometric technique has three advantages compared to gas source isotopic methods: (1) sample size requirements of this technique are 10-fold less permitting access to the higher resolution S isotope record of low concentration snow and ice, (2) the double spike technique permits $\delta^{34}S$ and S concentration to be determined simultaneously, and (3) the double spike is an internal standard.

1. INTRODUCTION

The formation of sulfate (SO_4^{2-}) aerosol particles in the atmosphere has important consequences for the biogeochemical cycling of sulfur (S) and global climate that are not fully understood. Sulfate aerosols interact *directly* with incoming solar and outgoing terrestrial radiation through scattering and absorption and *indirectly* function as cloud condensation nuclei that influence the concentration and size of droplets as well as their surface reflectivity, and the radiative properties of clouds (IPCC, 2001). Submicrometer aerosols, in particular, are efficient at scattering solar radiation because their dimensions are close to the wavelengths of visible light. The majority of these aerosols are derived from anthropogenic sulfur dioxide (SO_2) emissions. These submicrometer aerosols, which remain in the atmosphere for a few days to a week, influence atmospheric composition both downwind of industrialized areas and in remote areas of the world (Polian et al., 1986). Snow and ice cores archive the deposition of atmospheric SO_4^{2-} aerosols in cold, remote regions of the planet, including polar and high altitude temperate and tropical environments. Sulfur

* Corresponding author. Fax: +1 301 869 0413.
E-mail address: jmann@nist.gov (J.L. Mann).

0016-7037/$ - see front matter © 2008 Elsevier Ltd. All rights reserved.
doi:10.1016/j.gca.2008.05.036

isotope compositions of these aerosols can provide information on the degree of influence anthropogenic contributions have on the natural S cycle and ultimately on global climate.

The S isotope composition of remote marine and polar SO_4^{2-} aerosols sampled directly on filters has been used to identify source inputs to distant regions (Calhoun et al., 1991; Nriagu et al., 1991; Li et al., 1993; Norman et al., 1999; Patris et al., 2000b). The S isotope signatures of both shallow Antarctic ice cores and discontinuous Greenland ice core samples have been used to examine historical variations in SO_4^{2-} sources (Patris et al., 2000a, 2002; Pruett et al., 2004a,b). The SO_4^{2-} concentrations in these samples typically range from 25 to 150 ng/g. A major limitation of these studies was the need to combine large ice samples to obtain sufficient amounts of S to perform isotopic measurements by gas source isotope ratio mass spectrometry. The studies of Patris et al. (2000a, 2002), for example, required composite samples consisting of 1–6 kg of firn/ice mass (≈1–5 L of meltwater for densities of 0.5–0.9 g/mL) for analysis corresponding to a time interval of 3–8 years. The ability to resolve isotopic signatures at the annual and sub-annual level is required to better assess short duration point sources and discrete events.

The objective of this study is to demonstrate the capability of the recently developed double spike method (Mann, 2005; Mann and Kelly, 2005) for the simultaneous measurement of S isotope composition and SO_4^{2-} concentration in low-concentration (ng/g levels) snow samples to access the seasonal S isotope record preserved in snow pits. Higher resolution isotopic data can potentially provide not only a more detailed reconstruction of the dynamic atmospheric sulfur cycle on seasonal and sub-seasonal timescales in remote environments, but also expose the seasonal changes in the anthropogenic S source and the role these contributions play in the global S cycle and in climate forcing. Understanding the anthropogenic inputs to the S cycle is required to make informed environmental policy decisions. In addition, these types of measurements can provide additional data to test assumptions employed in atmospheric sulfur cycle models.

This paper describes the application of the new accurate and precise double spike technique and presents data for snow pit samples with ng/g SO_4^{2-} concentrations collected from two high-elevation locations (Inilchek Glacier, Kyrgyzstan and Summit, Greenland). The $\delta^{34}S$ data provide the first high-resolution (seasonal) continuous $\delta^{34}S$ profile from these regions, and are used in an isotope mass balance model to quantify the seasonal changes in the anthropogenic and natural S source contributions.

2. SAMPLING AND METHODS

2.1. Sampling scheme and protocols

Inilchek Glacier (42.16°N, 80.25°E, 5100 m) samples were collected by Kreutz and Sholkovitz (2000) from a snow pit of approximately 4 m depth in the summer of 2000. Approximately 1-L samples were collected from the Inilchek Glacier for $\delta^{34}S$ analysis at an interval of 20 cm. Samples from Summit, Greenland (72.58°N, 38.53°W, 3238 m) were collected by J.L.M. and C.A.S. from a snow pit of approximately 2 m depth in the Spring of 2001. Samples collected from Summit were taken every 10 cm (≈300 mL). Although it is possible to access the high-resolution record in snow pits using gas isotope ratio mass spectrometry by sampling laterally along a thin layer to obtain the required volume of sample for analysis, samples in this study were obtained in a manner similar to ice core samples to provide natural ("real") samples that are analogous to ice, but are easier and cheaper to obtain and are able to demonstrate and prove the capability of the new double spike technique for ice core research.

The two study sites were chosen for their high rates of accumulation and low rates of melting, sublimation, and condensation (Alley and Anandarkrishnan, 1995; Kreutz and Sholkovitz, 2000). These physical conditions minimize ion remobilization preserving the chemical and isotopic record. The rates of accumulation for the Inilchek range from 90 to 150 cm WE y^{-1} (Water Equivalent) (Kreutz et al., 2001; Kreutz et al., 2003; Aizen et al., 2004; Green et al., 2004) with most accumulation occurring in the summer months, while the accumulation rate for Summit is approximately 20 cm WE y^{-1} with continuous accumulation throughout the year (Johnsen et al., 1992; Shuman et al., 1995). Because of the relatively high accumulation rates, the snow pits offered a larger mass per unit time in which to test the new double spike method for $\delta^{34}S$ analysis of low (ppb level) SO_4^{2-} concentrations typical of these environments and to examine the potential seasonal changes in the S isotope record.

Separate depth profiles were taken for major ion concentrations, $\delta^{18}O$, and δD measurements. From the Inilchek, the depth profiles were taken at 5 cm resolution. Summit depth profiles were taken at 2 cm intervals for major ion measurements and at 3 cm for δD measurements. Samples were placed into pre-cleaned containers and packed in insulated shipping containers and transported frozen to the National Institute of Standards and Technology (NIST) and the Climate Change Institute at the University of Maine for processing. Samples were stored below −15°C until analysis. Major and minor ion (Na^+, K^+, NH_4^+, Mg^{2+}, Ca^{2+}, Cl^-, NO_3^-, SO_4^{2-}, and methane sulfonic acid) measurements for both the Summit and Inilchek snow pit samples were performed at the University of Maine using a dedicated Dionex DX-500 ion chromatograph (IC). Anions were analyzed with an AS-II column using 6 mM sodium hydroxide eluent and cations were analyzed with a CS-12 A column using 25 mM methane sulfonic acid eluent. The uncertainties for all species were ± 5% with the exception of SO_4^{2-} in the Summit samples which were ±20%.

$\delta^{18}O$ and δD measurements of the Inilchek Glacier samples were performed at the University of Maine. $\delta^{18}O$ measurements used the standard CO_2 equilibration technique of Epstein and Mayeda (1953) on a VG SIRA II mass spectrometer, and δD via continuous flow Cr reduction on a Micromass Isoprime mass spectrometer (Morrison et al., 2001). The analytical precision based on replicate analyses of samples and international standards for $\delta^{18}O$ is ±0.05‰ (1σ) and for δD is ±0.5‰ (1σ). Only δD measurements were performed on Summit samples and these were

carried out at the Institute of Arctic and Alpine Research (INSTAAR) at the University of Colorado, Boulder using an on-line hydrogen reduction technique combined with a Micromass SIRA Series II Dual Inlet mass spectrometer (Vaughn et al., 1998). The reproducibility on the δD measurements based on replicate analyses of multiple standard measurements was approximately ±0.3‰ (1σ). All data are reported in delta notation relative to Vienna Standard Mean Ocean Water (VSMOW).

2.2. Double spike

$\delta^{34}S$ and SO_4^{2-} concentration measurements were made simultaneously using a ^{33}S–^{36}S double spike specifically suited for the measurement of low SO_4^{2-} concentrations (Mann, 2005; Mann and Kelly, 2005). The technique is based on the production of singly charged arsenic sulfide molecular ions (AsS^+) by thermal ionization using silica gel as an emitter (Paulsen and Kelly, 1984) and uses the measured $^{33}S/^{36}S$ ratio, the double spike, to correct instrumental fractionation. The technique permits both $\delta^{34}S$ and S concentration to be measured with high precision. The technique is capable of a measurement precision of 0.1‰ or better on samples of ⩽1.5 μg S. Because of the low concentrations of SO_4^{2-} in snow and ice, $\delta^{34}S$ analysis by standard gas source techniques requires 300–4000 g of sample (≈33 μg S) (Patris et al., 2000a,b; Patris et al., 2002). Global atmospheric S cycling is a dynamic process that varies on short timescales thus using multi-year samples will mask seasonal and annual changes in S sources.

The isotopic composition and concentration of the ^{33}S–^{36}S double spike are given in Table 1. The details of spike preparation and calibration are in Mann and Kelly (2005). The 1:1 molar ratio $^{33}S/^{36}S$ spike was prepared from solutions of $^{33}SO_4^{2-}$ and $^{36}SO_4^{2-}$ that were prepared from enriched elemental S produced in Troitsk, Russia by TSD-Isotopes Limited. Ratio measurements of the double spike were corrected for both instrumental fractionation and blank to obtain a corrected isotopic composition. The double spike composition was calibrated against the Institute for Reference Materials and Measurement's absolute value for the standard IAEA-S-1 (International Atomic Energy Agency) $^{32}S/^{34}S = 22.6504$ (Ding et al., 2001). This procedure yields a double spike composition that is absolute relative to the IAEA-S-1 composition. The concentration of the spike was determined by calibrating it against a dilute solution prepared gravimetrically from Standard Reference Material (SRM) 3154 as described in Mann and Kelly (2005).

2.3. S processing/extraction/measurement

All sample handling was performed in a Class 10 laboratory. Prior to chemical processing samples were allowed to melt in their original low density polyethylene containers at room temperature. Based on sulfate concentrations determined by IC, aliquots were optimally spiked (molar ratio of 2; $R_{sample/spike} \approx 2$) with a weighed aliquot of the double spike. Addition of the spike at the beginning of the sample preparation process compensates for any mass fractionation produced during drying, chemical separation, and thermal ionization. This is a considerable advantage for small sample sizes (<1 μmol S) where losses could result in potentially large biases without the use of an internal standard. Samples were then dried on a hotplate in 250–400 mL Pyrex flasks with a 1 cm diameter 45° sidearm within a HEPA filtered glove box. This sidearm construction was designed to reduce particulate infall from the atmosphere thus reducing chemical blank. The solutions were heated to dryness under a flowing stream of argon (Ar) and samples were converted to the chloride form by the addition of 1 mL of high-purity HCl acid (Fisher Optima) and 4 mL of 18 MΩ MilliQ water and dried again. This step eliminates nitrates which can interfere with chemical reductions. The dried samples were dissolved in 1 mL of the high-purity HCl acid and 6 mL of 18 MΩ MilliQ water, and transferred to 30 mL polycarbonate bottles for storage until chemical reduction. Standards and high-concentration samples were processed in groups of four: 3 standards or samples and 1 blank. Low concentration samples were processed in groups of five: 2 samples, 2 standards (IAEA-S-1 and IAEA-S-2), and 1 blank. Blanks were prepared by adding a representative volume of 18 MΩ MilliQ water to a Pyrex flask and spiking with approximately 0.5 g of spike solution and dried as described above.

The chemical reduction and mass spectrometric procedures have been described previously in Paulsen and Kelly (1984) and Mann and Kelly (2005). Samples as small as 3 μg of S can be recovered using this technique. Yield experiments for this technique as performed by Paulsen and Kelly (1984) range from 73% to 90%.

Table 1
Sulfur concentration and atom abundances in % for the double spike

[S] (μmol/g)	^{32}S	^{33}S	^{34}S	^{36}S
0.6536 ± 0.0032 (2σ)	0.38	48.96	0.031	50.63

2.4. Data reduction

2.4.1. Instrumental mass fractionation correction

A nested iteration procedure was used to determine the $^{32}S/^{34}S$ isotopic ratios in the snow pit samples from the mass spectrometric measurements. It is similar to that used in previous double spike applications (Eugster et al., 1969; Russell et al., 1978; Todt et al., 1996; Johnson et al., 1999; Holmden, 2005). Full details of the technique including the basic derivation of the equations are in Mann and Kelly (2005). In this study, as in the previous studies, instrumental and natural fractionations were assumed to follow an exponential fractionation law. The sample $^{32}S/^{34}S$ ratio, prior to blank correction, is compared to the absolute natural composition for Vienna Canyon Diablo Troilite (VCDT) ($^{32}S/^{34}S = 22.6436$ (Ding et al., 2001), $\delta^{34}S = -0.3‰$) to calculate the natural $\delta^{34}S$ ($\delta^{34}S_m$) value for the sample using the following equation:

$$\delta^{34}S_m = \left[\frac{\left(\frac{^{34}S}{^{32}S}\right)_{sample}}{\left(\frac{^{34}S}{^{32}S}\right)_{VCDT}} - 1\right] \times 10^3 \quad (1)$$

where $\delta^{34}S_m$ is the instrumentally-corrected $\delta^{34}S$ value. See Table 2 for definitions of variables used in this and subsequent equations.

2.4.2. Blank correction and error propagation

The instrumentally-corrected $\delta^{34}S$ ($\delta^{34}S_m$) values calculated using the iterative scheme above may be biased due to blank contribution. Blank corrections were made using the formulation described by Hayes (2002). Using the following equations the instrumentally-corrected values derived from the iterative equations are blank-corrected to obtain the true $\delta^{34}S$ value:

$$\delta^{34}S_{bc} = \frac{\eta_m \delta^{34}S_m - \eta_b \delta^{34}S_b}{\eta_m - \eta_b} \tag{2}$$

and the variance of the correction procedure is calculated as:

$$\sigma^2_{\delta^{34}S_{bc}} = \frac{1}{(\eta_m - \eta_b)^2} \times \left[\left(\frac{\eta_b(\delta^{34}S_b - \delta^{34}S_m)}{\eta_m - \eta_b} \right)^2 \sigma^2_{n_m} + \eta_m^2 \sigma^2_{\delta^{34}S_m} \right] + \frac{1}{(\eta_m - \eta_b)^2} \times \left[\left(\frac{\eta_m(\delta^{34}S_m - \delta^{34}S_b)}{\eta_m - \eta_b} \right)^2 \sigma^2_{n_b} + (-\eta_b^2)\sigma^2_{\delta^{34}S_b} \right] \tag{3}$$

where m and b refer to measured and blank.

The uncertainty of the S isotope composition of the blank is a significant component of the error budget (Eq. (3)) as sample sizes decrease. In this work, $\delta^{34}S$ values for the blank were either directly measured or determined by mass balance calculations using offsets of standards from expected values, similar to that used to correct $\delta^{34}S$ values for scale contraction/expansion in gas source measurements. Scale contraction/expansion results from the mixing of two different gases of differing isotopic composition. In this work, two SO_4^{2-} samples (standard and blank or sample and blank) with differing S isotope composition are mixed to result in $\delta^{34}S$ values that deviate from the true value. Because the thermal ionization technique does not experience scale contraction/expansion, the assumption is that blank is the only cause for bias in $\delta^{34}S$ values. To determine the $\delta^{34}S$ value of the blank the following equation was used:

$$\delta^{34}S_b = a\delta^{34}S_m + b \tag{4}$$

where a and b are a factor and offset determined by the simultaneous solution of two equations that use the internally determined or raw $\delta^{34}S$ values determined for IAEA-S-1 and IAEA-S-2 and the instrumentally-corrected values for IAEA-S-1 and IAEA-S-2. All natural sample $\delta^{34}S$ values for this work fall within the range of these 2 standards. Using the uncertainties of the raw $\delta^{34}S$ values and the $\delta^{34}S_m$ values, 1000 points were produced using the Monte Carlo simulation. These points were then used to generate the a and b factors in Eq. (4) to determine an uncertainty for the blank composition. From this point for-

Table 2
Variable definitions for equations

Variable	Definition
$\delta^{34}S_m$	$\delta^{34}S$ value of sample or standard corrected for instrumental fractionation
$(^{32}S/^{34}S)_{sample}$	Mass 32/mass 34 ratio in the sample
$(^{32}S/^{34}S)_{VCDT}$	Mass 32/mass 34 ratio in the Vienna Canyon Diablo Troilite standard
$\delta^{34}S_{bc}$	The measured isotopic signature of SO_4^{2-} in the sample or standard which has been corrected for both instrumental fractionation and blank (true $\delta^{34}S$ value)
η_m	Amount of the measured sample or standard in micromoles derived from isotope dilution
η_b	Amount of the blank in micromoles derived from isotope dilution
$\sigma^2_{\eta_m}$	Concentration measurement uncertainty derived from the 1σ uncertainty on the measurements for the sample or standard
$\sigma^2_{\eta_b}$	Blank concentration uncertainty derived from the 1σ uncertainty determined from the pooled blanks run with each group of standards and samples
$\sigma^2_{\delta^{34}S_m}$	$\delta^{34}S$ measurement uncertainty derived from the external standard deviation (1σ) uncertainty for the standards or the samples (For the samples the standard deviation was derived from the pooled standard deviation for duplicate measurements. The resulting standard deviation was similar to that for the standards as the measurement precisions are the same if the signal intensities are similar)
$\sigma^2_{\delta^{34}S_b}$	$\delta^{34}S$ blank uncertainty either based on a best estimate from direct measurement assuming a 40‰ uncertainty (Mann and Kelly, 2005) or is derived from the 1σ uncertainty results from a Monte Carlo simulation described in Section 2.4.2.
$\delta^{34}S_b$	$\delta^{34}S$ value of the blank determined by either direct measurement or by the method described in Section 2.4.2.
a and b	Factor and offset determined by the simultaneous solution of two equations that use the internal absolute $\delta^{34}S$ values determined for IAEA-S-1 and IAEA-S-2 and the instrumentally-corrected $\delta^{34}S$ ($\delta^{34}S_m$) values for IAEA-S-1 and IAEA-S-2 (all natural sample $\delta^{34}S$ values for this work fall within the range of these 2 standards)
δ_{ss}, δ_{nss}, δ_a, δ_d, δ_{av}, and δ_{mb}	Isotopic signatures of the sea salt (ss), non-sea salt (nss), anthropogenic (a), dust (d), anthropogenic + volcanic (av), and marine biogenic (mb) components
f_{ss}, f_{nss}, f_a, f_d, f_{av}, and f_{mb}	Mass fractions of the sea salt (ss), non-sea salt (nss), anthropogenic (a), dust (d), anthropogenic + volcanic (av), and marine biogenic (mb) components
k	Mass ratio of SO_4^{2-} to Na^+

ward the $\delta^{34}S_{bc}$ notation indicates the value has been corrected for both instrumental fractionation and blank.

2.4.3. S concentration

A major advantage of the double spike MC-TIMS technique is that the isotopic composition and the concentration can be measured simultaneously in the same run. In addition method blanks can also be determined by isotope dilution (ID). The technique is inherently accurate because after the spike is mixed with the S in the sample only isotopic ratios need to be measured, and these ratios can be measured with high accuracy and precision. The accuracy is independent of chemical yields if corrected for fractionation. In this work, ^{33}S was the enriched isotope used and the $^{32}S/^{33}S$ fractionation corrected ratio was used to calculate $[SO_4^{2-}]$. All uncertainties are reported as expanded 95% confidence intervals.

2.5. Analytical precision

The analytical reproducibility of the technique was assessed by measuring two samples in triplicate. Three samples each collected from the Inilchek Glacier site during 2 separate fresh snowfall events on July 31 and August 3, 2000 were measured for $\delta^{34}S$ with results shown in Table 3. Because the samples were taken simultaneously, the $\delta^{34}S_{bc}$ values are expected to have the same or similar values within an individual snow event. The $\delta^{34}S_{bc}$ values ranged from +2.8‰ to +3.1‰ for the July 31st event and averaged $+3.0 \pm 0.3$‰ ($n = 3$) while the range for the August 3rd event was +2.3‰ to +2.4‰ and averaged $+2.4 \pm 0.1$‰ ($n = 3$). Uncertainties reported here are 2σ. The range in sample sizes used for these analyses was 0.10–0.65 μmol S. These tests demonstrate that the double spike technique is capable of precisions better than 0.3‰ (2σ) on sample sizes as small as 0.10 μmol S.

Small aliquots (23–75 μg) of solutions of isotopic standards IAEA-S-1 and IAEA-S-2 were carried through the complete chemical process with each group of samples. Table 4 gives the $\delta^{34}S_{bc}$ values and the corresponding sample size used for analysis. The reported $\delta^{34}S$ values for the standards were corrected for blank, which was determined to be from the silica gel and the As-NH_3 dilution solution used for loading (Mann and Kelly, 2005). The mean and standard deviation for IAEA-S-1 was -0.3 ± 0.3‰ (2σ), 0.1‰ ($2\sigma_m$) ($n = 8$) and for IAEA-S-2 was $+22.6 \pm 0.1$‰ (2σ), 0.05‰ ($2\sigma_m$) ($n = 6$). Both values agree with the consensus values (S-1 = − 0.3‰ and S-2 = $+22.7 \pm 0.3$‰ (2σ)) reported in Taylor et al. (2000) using sulfur hexafluoride (SF_6) techniques. In this study, the sample sizes used for analysis were about 10 times smaller (0.73–2.35 μmol S) than those used for $\delta^{34}S$ analysis by researchers employing gas source techniques (10–30 μmol S for IAEA-S-1, and 3–30 μmol for IAEA-S-2) (Taylor et al., 2000). From this point forward all uncertainties reported for $\delta^{34}S$ composition measurements are 2σ unless stated otherwise.

Table 3
Repeat $\delta^{34}S$ measurements for two separate fresh snow events (Inilchek Glacier)

Snow event	$\delta^{34}S$ (‰ VCDT)[a]	Sample size (μmol S)[a]
July 31, 2000	2.8	0.60
	3.1	0.65
	3.0	0.63
Average ($n = 3$)	**3.0**	
2σ	**0.3**	
August 3, 2000	2.4	0.23
	2.4	0.13
	2.3	0.10
Average ($n = 3$)	**2.4**	
2σ	**0.1**	

The bold values are to highlight the average and 2σ standard deviation.
[a] Values are blank corrected.

Table 4
Summary of reproducibility of $\delta^{34}S$ measurements for IAEA-S-1 and S-2

Standard	Consensus value (‰ VCDT)	$\delta^{34}S$ (‰ VCDT)[a]	2σ	Sample size (μmol S)	n
IAEA-S-1	−0.3	−0.31	0.26	0.73–2.35	8
IAEA-S-2	$+22.7 \pm 0.3$ (2σ)	22.60	0.12	1.03–1.22	6

[a] Values are blank corrected.

3. ATMOSPHERIC SULFUR SOURCES FOR THE TWO SITES

3.1. Inilchek Glacier

The S budget of the Inilchek Glacier is dominated by evaporite dust and anthropogenic S inputs (Pruett et al., 2004a) (Fig. 1). Significant fluxes of evaporite dust (gypsum—$CaSO_4 \cdot 2H_2O$) come from a deposit in Central Asia that lies between the Aral and Caspian Seas (Fig. 1) (Wake et al., 1994; Kreutz and Sholkovitz, 2000; Kreutz et al., 2001; Pruett et al., 2004a). Modeling by Claquin et al. (1999) indicates that the area surrounding the Caspian and Aral Seas is the largest source of soil gypsum in the world. Prevailing synoptic meteorological conditions favor west to east transport of this S dust to the Inilchek site (Aizen et al., 1996, 1997; Claquin et al., 1999; Aizen et al., 2004). Kreutz and Sholkovitz (2000) suggest that loess dust sources of S are also delivered to this site from the south (China) based on examination of major element and rare earth elements of mineral dust; yet this source is far exceeded by the non-loess (evaporite) sources. Contributions directly from marine sources are negligible due to the long distance from a seawater source as demonstrated by the major ion ratios and the synoptic meteorology (Wake et al., 1990, 1992; Kreutz et al., 2001; Pruett et al., 2004a). Volcanic source contributions are insignificant as there are no known volcanic centers in this region. Additionally, no evidence exists in the regional Asian ice core record of other major global volcanic events (e.g., Agung, Krakatau, Tambora) (Kang et al., 2002; Pruett et al., 2004a). Moreover, there is no indication of global-scale explosive activity during 2000, the period in which the samples for this study were collected. Continental biogenic sources of S in the region are likely to be insignificant given the aridity of the surrounding region. Previous researchers

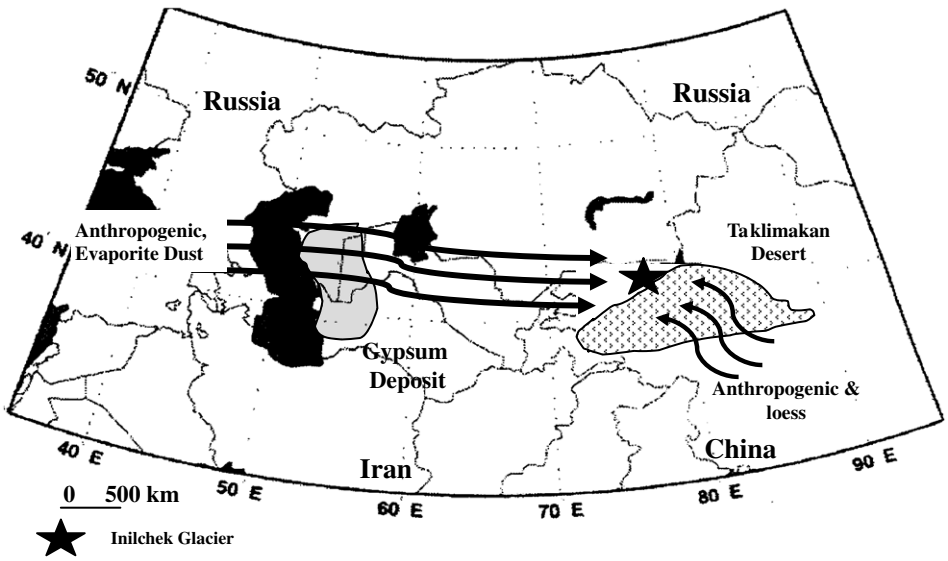

Fig. 1. Location of the major S sources (anthropogenic and evaporite dust) contributing to the Inilchek Glacier. The black arrows highlight the transport directions, inferred from the synoptic meteorology, considered to be responsible for delivering SO_4^{2-} to the region (Wake et al., 1994; Aizen et al., 1996, 1997, 2004; Claquin et al., 1999; Kreutz and Sholkovitz, 2000; Kreutz et al., 2001). Figure modified after Kreutz and Sholkovitz (2000).

have noted the lack of methane sulfonic acid in Asian snow (Wake et al., 1992, 1994) for which marine biogenic emissions are the only source. The remaining fraction of the S budget of the Tien Shan region is attributed to anthropogenic origins. Previous work has suggested that anthropogenic S from Russia and the countries of the Former Soviet Union as well as China may be significant S sources impacting the snow chemistry in the region (Wake et al., 1992; Kreutz and Sholkovitz, 2000; Pruett et al., 2004a). These regions include major industrial centers and are likely contributors of anthropogenic S to the Inilchek site based on the local- to regional-scale atmospheric circulation for the region. Pruett et al. (2004a) estimated that 60% of the deposited SO_4^{2-} during the 1999 summer season was from an evaporite source and the remaining was from anthropogenic sources. They also determined that anthropogenic SO_4^{2-} dominates during "background" periods—periods without high dust deposition.

The $\delta^{34}S$ values determined in this study are used to test the fractional estimates from the earlier Pruett et al. (2004a) study. Sulfates derived from Asian evaporite deposits have $\delta^{34}S$ values ranging from +11‰ to +36‰ (Krouse and Grinenko, 1991). The range is typical of that observed for seawater SO_4^{2-} through geologic time (Claypool et al., 1980) encompassing the modern marine sulfate $\delta^{34}S$ value of $+21 \pm 0.2$‰ (Rees et al., 1978). Specific $\delta^{34}S$ data for the evaporite deposits located near the Aral and Caspian Seas do not exist; for the mass balance calculations of this study we assume an average value of +20‰. $\delta^{34}S$ values of industrial S materials (e.g., fossil fuels and sulfide ores) range from −40‰ to +30‰ (Nielsen, 1974; Newman et al., 1991); although regionally, individual though related deposits can have a relatively uniform isotopic composition (Wedepohl, 1978). The anthropogenic sulfate delivered to the Tien Shan region is largely from the surrounding industrialized countries. The $\delta^{34}S$ values of Russian oil deposits are typically <+10‰ and coal deposits are <0‰ (Wedepohl, 1978) and most sulfide ore deposits lie within −3‰ to +5‰ (Krouse and Grinenko, 1991). Limited $\delta^{34}S$ data is available for these same sulfur-bearing materials indigenous to China. Mukai et al. (2001), however, found that the average $\delta^{34}S$ value for SO_2 and SO_4^{2-} in the atmosphere over China was similar to the coals used, suggesting coal combustion is a large contributor of S to the atmosphere. The $\delta^{34}S$ of precipitation SO_4^{2-} sampled from northern cities was about +5‰ while that from the southern city of Guiyang was approximately −3‰, which is representative of coals from southern China that have unusually light S isotope ratios. Sulfate in precipitation from urban regions surrounding the Inilchek reflect the isotopic composition of the fossil fuels used and appear to fall in the −5‰ to +5‰ range. Because the predominant fossil fuel sources from these industrialized regions have $\delta^{34}S$ values that tend toward lighter values, a signature of near 0‰ is likely.

3.2. Summit

The S budget for central Greenland today is dominated by S from anthropogenic source contributions (Fig. 2). Anthropogenic sulfur emissions have been increasing since the late 19th century surpassing natural emissions in the northern hemisphere by about 1910 (Dignon and Hameed, 1989; Lefohn et al., 1999) and on a global scale during the 1950s (Spiro et al., 1992). This historical trend is documented in Greenland ice cores where increasing non-sea salt (nss) SO_4^{2-} levels have been recorded for over one hundred years coincident with industrial activity (Neftel et al., 1985; Finkel et al., 1986; Mayewski et al., 1986; Mayewski et al., 1990; Legrand et al., 1997; Legrand and Mayewski, 1997; Patris et al., 2002) from an average of 22 ppb (1870–1900) to 84 ppb (1968–1984). Anthropogenic contributions to SO_4^{2-} deposited at Summit are primarily derived from Eur-

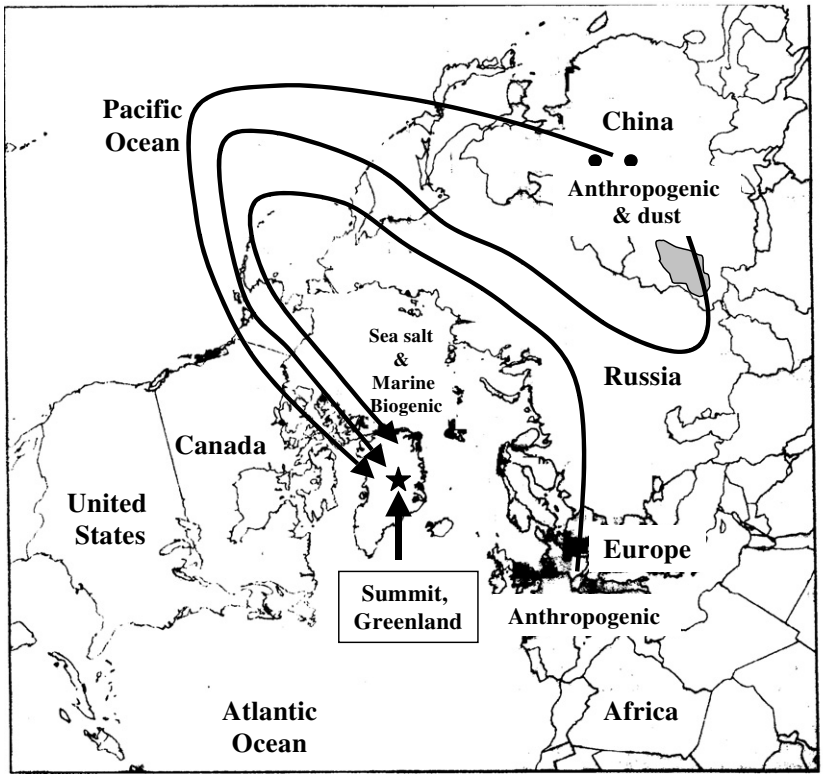

Fig. 2. Location of the major S sources (sea salt, marine biogenic, anthropogenic, and dust) contributing to Summit. The black arrows highlight the dominant transport directions responsible for delivering anthropogenic and dust S to the region (Christensen, 1997). Sea salt and marine biogenic are from local (Atlantic) sources. Figure modified after Christensen (1997).

asia where a persistent anticyclone over northern Asia in both winter and spring forces some of the air pollution from Europe and Russia to the Arctic Region (Christensen, 1997). Sources other than anthropogenic contributing SO_4^{2-} to the Summit site include volcanic, eolian, marine biogenic, and sea salt (Fig. 2). Background volcanism, including non-eruptive and weakly eruptive degassing, also contributes to the Greenland S budget (Legrand et al., 1997). These volcanic events are not clearly marked by the high acidity and nss-SO_4^{2-} levels observed with eruptive volcanic contributions, but are dilute enough to be incorporated into the background SO_4^{2-} levels indicating they represent a small portion of the overall S budget for the region. During the time period covered by this snow pit there were no explosive volcanic events and global non-eruptive SO_4^{2-} contributions are small relative to the total anthropogenic S being emitted to the atmosphere (<6.5%) (Koch et al., 1999; Barth et al., 2000; Chin et al., 2000a,b; Rasch et al., 2000). The main source regions of dust reaching Summit are from the Takla Makan desert and the inner Mongolian deserts of northern China, including the Tengger and Mu Us (Biscaye et al., 1997; Bory et al., 2002; Bory et al., 2003a,b). Dust inputs from the Takla Makan dominate during the dusty spring months while those from the Tengger and Mu Us dominate during the remainder of the year (Bory et al., 2003b). Both marine biogenic SO_4^{2-} produced from dimethylsulfide oxidation and sea salt SO_4^{2-} are regionally-derived. Using isotopic compositions to estimate source contributions Nriagu et al. (1991) were the first to provide constraints on the S isotopic composition of aerosol SO_4^{2-} in the Arctic at Alert and Mould Bay, Canada. They determined that in the winter industrial S emissions account for the majority of the airborne flux while in the summer months contributions from sea salt and marine biogenic sources increasingly become more significant. A recent study by Wasiuta et al. (2006) found similar results for the Prince of Wales icefield in Ellesmere Island, Canada. More specifically, Li and Barrie (1993) found summer aerosol SO_4^{2-} at the Alert, Canada site was 25–30% marine biogenic, 1–8% sea salt and 62–74% anthropogenic in origin. At other times of the year the sea salt contribution remained constant (1–8%), yet marine biogenic sources were <14% and the remainder were from anthropogenic sources. Norman et al. (1999) found similar results to Li and Barrie (1993) for the Alert site with the sea salt fraction averaging 5% and the marine biogenic fraction contributing on average 30% during the summer months. In addition, although the Norman et al. (1999) study did not distinguish between soil and anthropogenic sources, they suggested that during the fall and winter months the decreasing $\delta^{34}S$ values they observed were due to the increase in anthropogenic pollution inputs.

Mass balance arguments based on stable S isotope compositions of snow pit SO_4^{2-} are similarly used here to determine the primary S contributors to the Summit, Greenland region. The isotopic composition of marine biogenic SO_4^{2-} lies between +14‰ and +22‰ (Calhoun et al., 1991), which is close to that of sea water (+21 ± 0.2‰ (1σ), Rees et al.,

1978). Sulfate aerosols collected from above the Atlantic and Pacific oceans have isotope compositions that fall within this range (Calhoun et al., 1991; Patris et al., 2000b); however, Patris et al. (2000b) suggested that the lighter values could be influenced by S sourced from weathered sulfide minerals in continental soils. Based on the measurement of background SO_4^{2-} contained in snow at the South Pole, which is dominated by marine biogenic inputs and void of continental influences, Patris et al. (2000a) suggested that a $\delta^{34}S$ value of $+18.6 \pm 0.9‰$ (1σ) is a better estimate of the marine biogenic component. Anthropogenic S has been shown to have large isotopic variability; yet, in atmospheric and precipitation samples, $\delta^{34}S$ values tend to be in the range of 0‰ to +7‰ (Cortecci and Longinelli, 1970; Saltzman et al., 1983; Nriagu et al., 1987; Li and Barrie, 1993; Herut et al., 1995; McArdle and Liss, 1995; Wadleigh et al., 1996; Ohizumi et al., 1997; McArdle et al., 1998; Pichlmayer et al., 1998; Norman et al., 1999; Querol et al., 2000). For the Summit location, Patris et al. (2002) identified values of $+2.5 \pm 1.3‰$ to $+3.0 \pm 1.6‰$ (1σ) for three 20th century samples, which fall within the range typically observed for anthropogenic S. These values are slightly depleted relative to the +5‰ values observed for anthropogenic S delivered during Arctic Haze events (Norman et al., 1999). The mid range $\delta^{34}S$ value of +3‰, including the uncertainties, is likely the best estimate for the isotopic signature of the anthropogenic source for Summit. Volcanic S emissions have also been shown to be quite variable having $\delta^{34}S$ values ranging from −10‰ to +10‰ (Nielsen et al., 1991). This spread, however, is reduced to a range of 0‰ to +5‰ with mixing over large scales by atmospheric transport (Newman et al., 1991). Gaseous emissions from non-eruptive volcanic activities, such as for the time period represented by the snow pits in this study, are found to be quite uniform at $+2.6 \pm 0.3‰$ (1σ) (Newman et al., 1991) and $+2.5 \pm 2.5‰$ (1σ) (Patris et al., 2000a). The isotopic signatures for the dust sources reaching Summit (Takla Makan desert and the inner Mongolian deserts) are unknown but may fall within the range characteristic of sedimentary sulfides and sulfates (Nielsen et al., 1991). It is estimated that the flux of S from dust sources is approximately 20 Tg S y^{-1} (Brimblecombe et al., 1989); this accounts for <10% of the total global sulfate budget.

4. RESULTS AND DISCUSSION

4.1. Snow pit age assignments using D/H and $^{18}O/^{16}O$ ratios

4.1.1. Inilchek

$\delta^{18}O$ and δD values from the Inilchek snow pit range from −8.7‰ to −27.1‰ and −29.6‰ to −200‰, respectively, and are highly correlated (Fig. 3 and Table EA-1). The range in values observed is comparable to other snow pits from this region. Firn cores previously obtained from this location show a clear seasonal trend in $\delta^{18}O$ with values typically higher than −20‰ in the summer and values as low as −35‰ in winter (Kreutz et al., 2001, 2003). The snow pit in this study shows two isotopic minima, at 170 and 365 cm depths where the $\delta^{18}O$ values reach −27.1‰, and two broad maxima where values approach −8.7‰.

Estimates of accumulation rates determined from glaciological studies for this location are quite variable both on average for the time periods represented and from year-to-year. Green et al. (2004) determined the average accumulation rate over approximately 50 years averaged 163 cm WE y^{-1} based on the ^{36}Cl profile (Green et al., 2004); assuming a density of 0.5 this represents 325 cm of snow. Similarly, the accumulation rates estimated from the stable isotope profiles from both an 18 m core recovered in 2000 (Kreutz et al., 2003) and a shallow firn core from 1998 (Kreutz et al., 2001) were approximately 150 cm WE $y^{-1}$for 1994–2000 and 146 cm WE y^{-1} for 1992 to 1998, respectively. However, regional meteorologic studies (Aizen et al., 1997, 2004) calculated a lower mean annual snow accumulation of 116 cm WE y^{-1} (roughly 200–240 cm of snow) for the 1992–1998 period. Accumula-

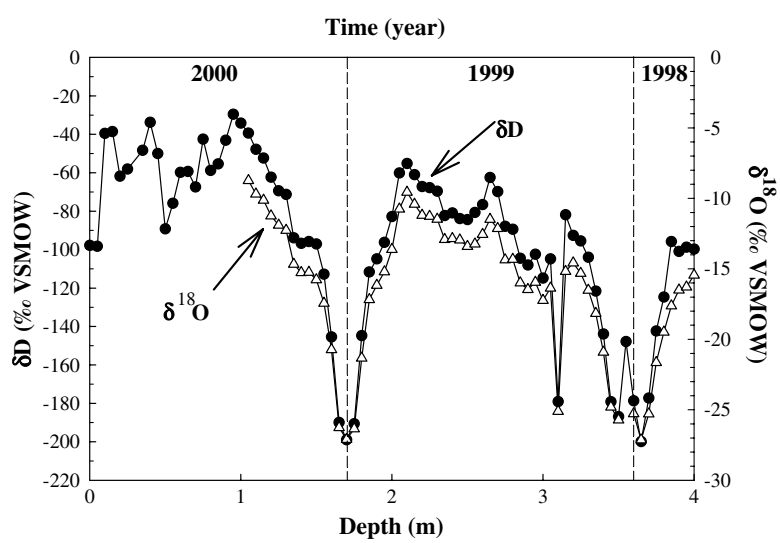

Fig. 3. δD (solid circles) and $\delta^{18}O$ (open triangles) data used to date the 2000 Inilchek snow pit. δD and $\delta^{18}O$ uncertainties are ±0.5‰ and ±0.05‰, respectively. Vertical dashed lines mark the year. VSMOW, Vienna Standard Mean Ocean Water. Error bars are smaller than the symbols. The collection date for this snow pit was August 4, 2000.

tion rates determined by Aizen et al. (2004) for 1992 and 1995 were lower than average at approximately 100 cm WE y^{-1} and 90 cm WE y^{-1}(roughly 160–180 cm of snow), respectively. Recognizing the potential for significant variability in accumulation rates for this region and the fact that the snow pit samples in this study were obtained in August of 2000, the occurrence of the next winter layer (Winter 1999/2000) at 170 cm (85 cm WE y^{-1}) is permissable. In fact, Aizen et al. (2004) calculated a similar rate of accumulation, 77 cm WE y^{-1}, for the same period in 1998. The amount of snow accumulation to the next winter layer at 365 cm is 195 cm, which corresponds to approximately 100 cm WE y^{-1}; identical to the accumulation rate in 1992 determined by Aizen et al. (2004). Based on the isotopic records and the previously identified accumulation rates, the snow pit likely represents precipitation occurring over approximately a 22-month period. The samples taken for S isotopic analysis, therefore, provide a continuous $\delta^{34}S$ record from winter 1998/1999 to August of 2000. An estimate of the age uncertainty for this profile is 1–3 months as matching profiles to other snow pits is difficult (Fisher et al., 1985, 1996; White et al., 1997).

4.1.2. Summit

The dating technique used for the Greenland snow pit is discussed in Shuman et al. (1995, 1998). The technique relies on the relationship of the stable isotope depth series (in this study δD) to surface temperature at a site. The δD record is a proxy for the surface temperature record assuming accumulation occurs relatively consistently throughout the year, which is the case at Summit. Comparison is made between the proxy temperature δD record and the actual surface temperature record obtained from an automatic weather station located approximately 1 km from the field site using a qualitative point-pairing technique that is directed by the maxima, minima, and inflections in the shape of the profiles. The surface temperature for the snow pit ranged from 224 to 263 K, with the temperatures above 250 K occurring in the summer months, May through September, and the temperatures below 240 K occurring in the winter months, between November to March (Fig. 4a). δD values in the snow pit ranged from −319‰ to −176‰ (Fig. 4b and Table EA-2) and fall within the δD range identified previously, −350‰ to −200‰ (cf. Shuman et al., 1995). δD values in the summer months are generally above −230‰ and in the winter months below −250‰. Based on the distinct seasonal trend in both records, the snow pit extends back approximately 21 months representing an essentially continuous $\delta^{34}S$ record from mid-August 1999 to the beginning of May 2001. The uncertainty in the ages is approximately ±2 weeks.

4.2. Concentration and S isotope results

4.2.1. Inilchek

$\delta^{34}S_{bc}$ values and the corresponding total SO_4^{2-} concentration data in time (depth) series for the Inilchek samples are shown in Fig. 5. The range in $\delta^{34}S_{bc}$ values is from

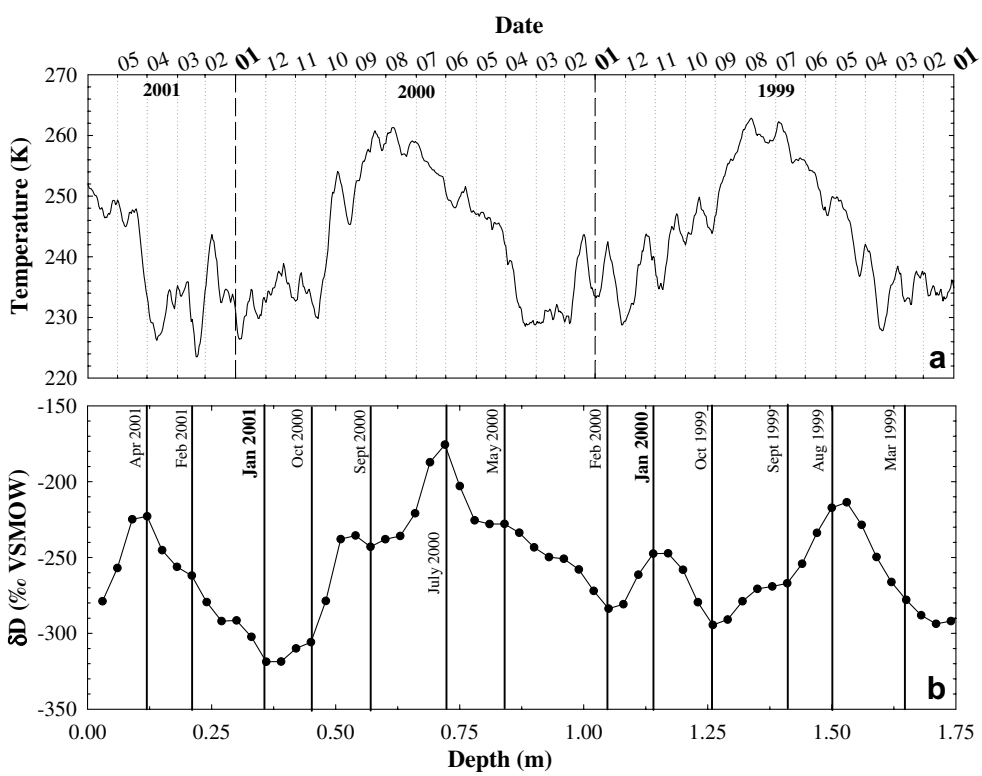

Fig. 4. (a) The composite temperature record (14 day average) from the automatic weather station (AWS) (72.58°N, 38.50°W) and (b) the δD record used to link the depth profile with time for the Greenland snow pit. The solid vertical lines in (b) highlight time. The surface of the snow pit (0 m) marks the date the snow pit was dug (May 7–8, 2001). Uncertainties for the δD and temperature measurements were ±0.3‰ (1σ) and ±2 K (1σ). VSMOW, Vienna Standard Mean Ocean Water.

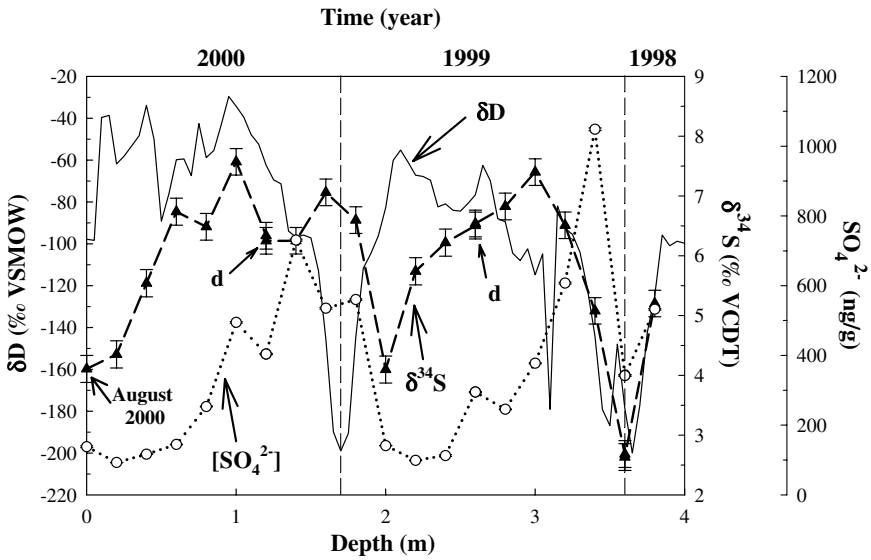

Fig. 5. $\delta^{34}S_{bc}$ values (solid triangles) and corresponding SO_4^{2-} concentration data (open circles) in time (depth) series for the Inilchek snow pit. Small letter d's indicate duplicate analyses. Vertical dashed lines mark the year. $\delta^{34}S$ uncertainties are 2σ and SO_4^{2-} concentration uncertainties, which are smaller then the symbol size, are 95% CI. VSMOW, Vienna Standard Mean Ocean Water; VCDT, Vienna Canyon Diablo Troilite.

$+2.6 \pm 0.40‰$ to $+7.6 \pm 0.40‰$ and averaged $+5.8‰$ for sample sizes ranging from 0.26 to 1.82 μmol S. Total SO_4^{2-} concentrations determined by ID ranged from 92.6 ± 0.4 to 1049 ± 4 ng/g. The amount of meltwater used for S isotope and concentration analysis ranged from 138 to 358 mL, and averaged 205 mL. We obtained high-resolution $\delta^{34}S$ (≈9 samples/year) with each analysis representing about 1.5 months. It is important to note that one liter samples were originally collected for gas source analysis. Therefore, even though higher resolution is possible with the double spike technique, the resolution of this record is consistent with that of 1 L of meltwater. The procedural analytical blank for this portion of the study was quite low and averaged 90 ± 51 ng S (2σ) for the larger sample sizes (0.43–1.82 μmol) and 100 ± 170 ng S (2σ) for the smaller sample sizes (0.26–0.43 μmol). The chemical blank composition determined using Eq. (4) was $+8.8 \pm 0.1‰$.

The ID and IC SO_4^{2-} concentration results are both plotted versus depth in Fig. 6. There is a clear systematic offset between the data which points to potential problems such as dilution or calibration issues. ID concentration values of gravimetrically prepared control samples (standards IAEA-S-1 and S-2) measured using a previously prepared spike agree with the concentration results obtained with the spike in this study. In addition, SRM 2724b (sulfur in Diesel Fuel Oil, 0.04%) was also measured with the previously prepared spike and the values were in excellent agreement with the certified value. We have confidence in the ID

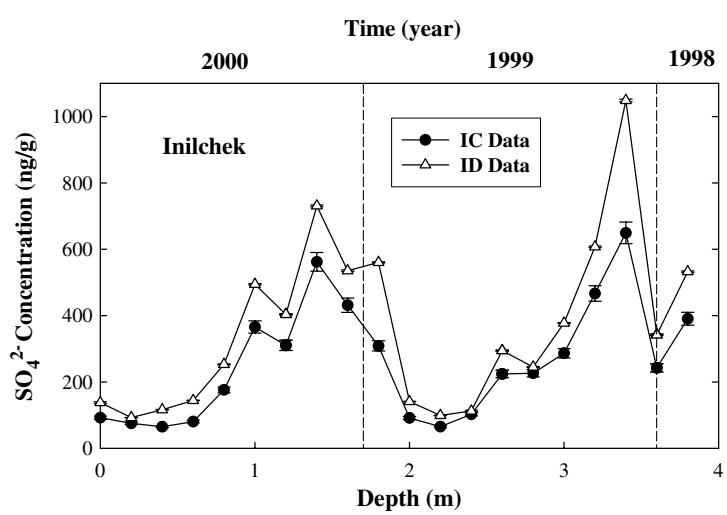

Fig. 6. Ion chromatograph and ID concentration data for the Inilchek (a) samples. Uncertainties are ±5% for the IC data and 95% CI for the ID data.

results. The IC sulfate data were used as an approximate concentration for spiking purposes only.

The $\delta^{34}S_{bc}$ values as well as SO_4^{2-} concentrations observed appear to show a discernable seasonal trend not observed in previous studies (Fig. 5). The $\delta^{34}S_{bc}$ values cover a limited range ($\approx +5‰$) with the more ^{34}S-enriched values observed in winter and spring of 1999 and 2000 (maximum at 1.0 and 3.0 m) and more ^{34}S-depleted values in the summer and fall months (minima at 2.0 and 3.6 m). All values lie below $+10‰$ and are similar to the range seen in the 1999 Inilchek snow pit where most values, with the exception of a single high value ($\approx +13‰$) attributed to evaporite dust input, were typically $< +10‰$ (ranging from $+1‰$ to $10‰$) (Kreutz and Sholkovitz, 2000; Pruett et al., 2004a). The SO_4^{2-} concentration results show two peaks in concentration, at approximately 1.4 m (731 ± 3 ng/g) and 3.4 m (1049 ± 4 ng/g), and two minima at 0.2 m (92.6 ± 0.4 ng/g) and 2.2 m (99 ± 1 ng/g). Concentrations for other major ion species (Na^+, Mg^{2+}, K^+, Ca^{2+}, NH_4^+, Cl^-, and NO_3^-) similarly peak and reach a minimum at the same depths, with the exception of NH_4^+ which decreases at 3.4 m (Fig. 7) suggesting that two years are represented by this core. All concentration data are comparable to the ranges found both in a firn core recovered in 1998 and snow pit samples collected in the summer of 1999 from the Tien Shan region (Kreutz and Sholkovitz, 2000; Kreutz et al., 2001; Aizen et al., 2004; Pruett et al., 2004a). Typically the snow pit major ion chemistry, including $[SO_4^{2-}]$ from the Tien Shan region have shown a pattern of low concentration intervals punctuated by episodic increases in ion concentration (Wake et al., 1992; Kreutz and Sholkovitz, 2000; Kreutz et al., 2001; Pruett et al., 2004a). Kreutz and Sholkovitz (2000) and Kreutz et al. (2001) attributed this pattern to a significant flux of evaporite dust coming from central Asia. The snow pit chemistry record here, however, does not exhibit any obvious dust events as evidenced by the lack of large spikes in SO_4^{2-} concentrations, suggesting only "background" contributions of dust, but does show broad minima and maxima which appear to follow seasonal trends.

The $\delta^{34}S_{bc}$ and SO_4^{2-} concentration data profiles are poorly correlated ($r = 0.16$) in strong contrast to the

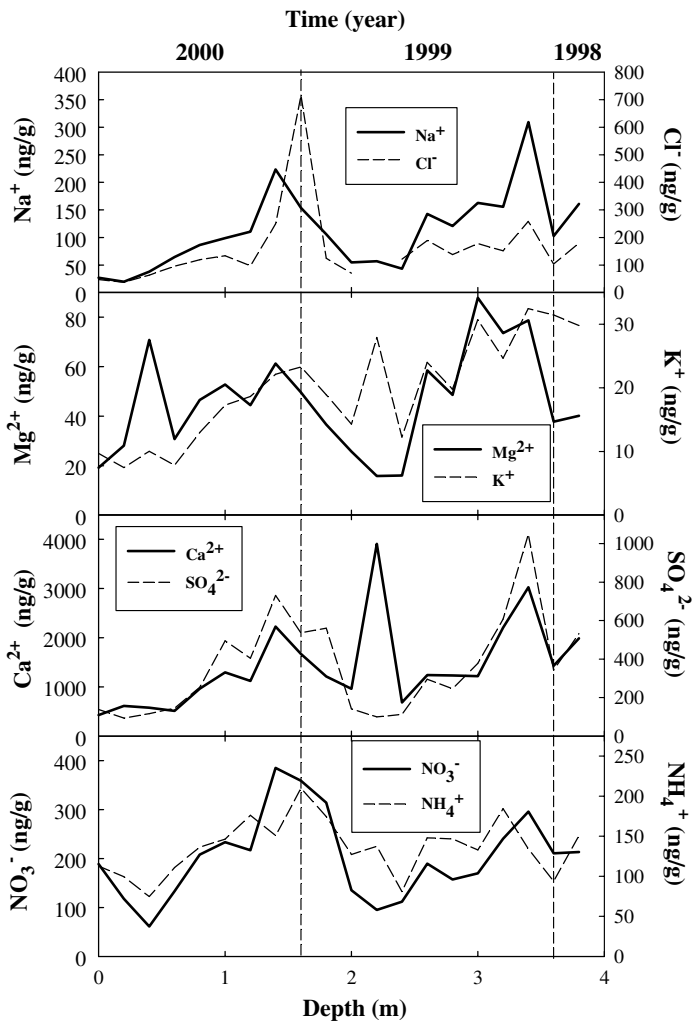

Fig. 7. Concentration data for major ions in time (depth) series for the Inilchek snow pit. Vertical dashed lines mark the year. All data shown were determined by IC (Uncertainties = ±5%) except for the SO_4^{2-} data which was determined by ID (Uncertainties are expressed as 95% CI).

findings of Pruett et al. (2004a) who found a significant positive correlation ($r = 0.87$) for the 1999 Inilchek snow pit. However, the regression of the data determined in that study was largely controlled by a single high value (represented by a high SO_4^{2-} concentration of 1440 ng/g) with an enriched $\delta^{34}S$ value of +13‰. Regression of only the low concentration samples yields a poor correlation, as observed in this study, suggesting these samples are also likely representative of "background" flux conditions. The majority of the $\delta^{34}S$ values determined for the 1999 snow pit (+1‰ to +10‰) were less enriched in ^{34}S and closer to the signature value of the anthropogenic component near 0‰. Similarly, a low SO_4^{2-} concentration and lighter $\delta^{34}S$ value (+5.4‰) sample, lighter relative to the evaporite dust component, identified in a firn core collected in 1998 was also attributed to anthropogenic sources. These studies suggest that under "background" conditions anthropogenic S sources tend to dominate. All the $\delta^{34}S$ values in the snow pit collected for this work are ^{34}S-depleted (+2.6‰ to +7.6‰) relative to evaporite dust, and are closer in value to the anthropogenic component than the evaporite dust component assumed to be +20‰. The poor correlation between $\delta^{34}S_{bc}$ and SO_4^{2-} concentration and the lighter $\delta^{34}S$ values of this snow pit appear to suggest that anthropogenic inputs dominate during "background" conditions.

4.2.2. Summit

The $\delta^{34}S_{bc}$ results and the corresponding total SO_4^{2-} concentration data for the Summit samples are shown in Fig. 8. The range in the $\delta^{34}S_{bc}$ values is $+3.6 \pm 0.7$‰ to $+13.3 \pm 5$‰, and is slightly larger than that of the Inilchek samples. Sample sizes used for analysis here ranged from 0.05 to 0.29 μmol S. The concentrations for total SO_4^{2-} determined by ID were an order of magnitude smaller than the concentrations observed for the Inilchek samples and ranged from 18 ± 9 to 93 ± 6 ng/g. The uncertainties for the ID data are larger than for the IC results because of the relatively large blank contribution in the former, but overall results are still in good agreement (Fig. 9). The amount of meltwater used in this study ranged from 209 to 307 mL, which is considerably less than the 1–2.5 L used by Patris et al. (2002) for analysis of samples from the same region.

The average blank for the Summit samples was 545 ± 417 ng S (2σ), which is a factor of 5.5 larger than the average blank concentration obtained for the Inilchek samples. These high blanks are atypical relative to both the standards and the Inilchek samples. Although the cause of this larger blank has not been identified, it may be related to a change in argon gas suppliers. The blank isotopic composition determined using Eq. (4) was -0.4 ± 0.3‰. The blank uncertainty was approximately a factor of two larger than the uncertainties for the Inilchek samples. Consequently, the relatively large blanks combined with the smaller sample sizes resulted in larger uncertainties (0.7‰ to 5‰) for the Summit samples, and only the extreme $\delta^{34}S_{bc}$ values are distinguishable from each other. It is important to note that the $\delta^{34}S$ measurement precisions after correction for instrumental fractionation ranged from 0.3‰ to 1‰ and were up to a factor of 5 better than the precisions obtained after correction for blank. This demonstrates that the blank was clearly the cause of the degraded precisions for these samples.

The $\delta^{34}S_{bc}$ values show a seasonal trend similar to that observed in previous studies for other Arctic regions and to that observed in the Inilchek snow pit (Fig. 8). The range in $\delta^{34}S_{bc}$ values was approximately 10‰, with more ^{34}S-enriched values observed in the summer and more ^{34}S-depleted values occurring in the winter and spring months. The range in $\delta^{34}S$ values (+3.8‰ to +8.0‰) observed for Summit samples covering the industrial period collected by Patris et al. (2002) falls within that observed here. Overall, the range for the samples in this study is twice

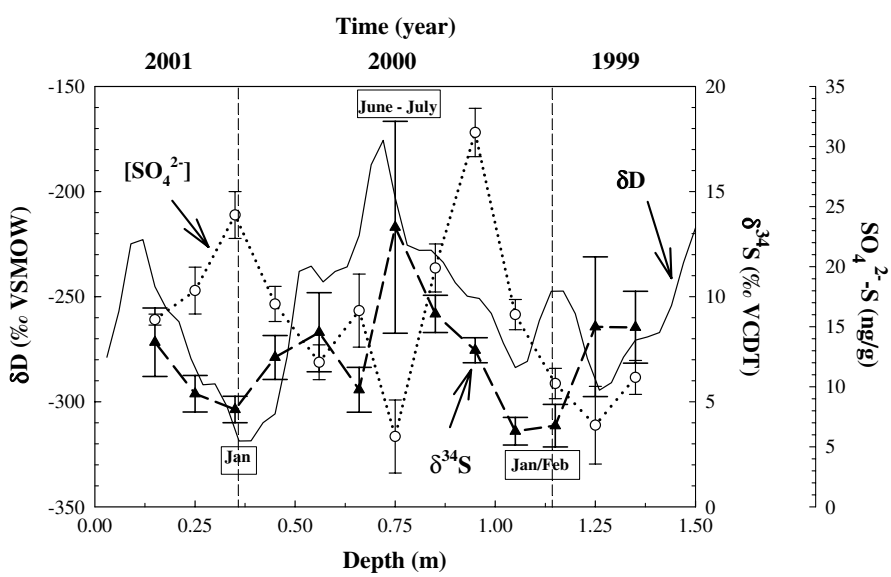

Fig. 8. $\delta^{34}S_{bc}$ (solid triangles) values and corresponding SO_4^{2-} (open circles) concentration data in time (depth) series for the Greenland snow pit. Vertical dashed lines mark the year. Dates in the boxes highlight extremes in $\delta^{34}S$ values. Uncertainties are 2σ and SO_4^{2-} concentration uncertainties are 95% CI. VSMOW, Vienna Standard Mean Ocean Water; VCDT, Vienna Canyon Diablo Troilite.

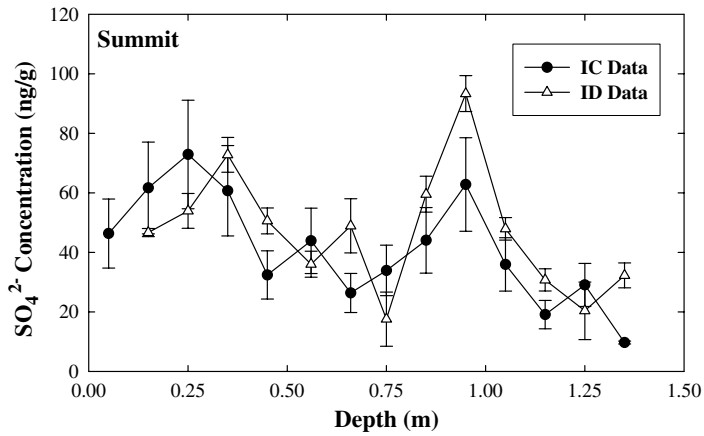

Fig. 9. Ion chromatograph and ID concentration data for the Summit samples. Uncertainties are ±5% for the IC data and 95% CI for the ID data.

that of Patris et al. (2002). The samples collected by Patris et al. (2002) covered 3–4 years of time; consequently, the small range in $\delta^{34}S_{total}$ observed (4‰) may result from the comparatively long averaging time that masks seasonal extremes in $\delta^{34}S$ values. The heavy $\delta^{34}S_{bc}$ value (+13.3‰) is similar to the heavy values seen by Patris et al. (2002) for samples representative of the pre-industrial background (average = +10‰) that were attributed primarily to marine biogenic and volcanic S inputs. The lighter $\delta^{34}S_{bc}$ values (+3.6‰, +3.9‰, and +4.6‰) of the winter and spring months are similar to the lighter value (+3.8‰) observed by Patris et al. (2002) for a sample taken in 1967, which may reflect a progressive trend toward lighter values associated with increasing anthropogenic S emissions. Sea salt and dust inputs have apparently changed little from pre-industrial to industrial times as evidenced by the negligible changes in the Na^+ and Ca^{2+} mean concentrations (Legrand et al., 1997); therefore, the majority of the variability observed in the $\delta^{34}S$ values of this study is likely due to changes in the anthropogenic and marine biogenic sources.

The total SO_4^{2-} concentrations also exhibit clear seasonality, with concentrations peaking during the winter and spring months at approximately 0.4 m (73 ± 6 ng/g) and just below 1 m (93 ± 6 ng/g) (Fig. 10). This seasonal trend in SO_4^{2-} concentration has been observed since the commencement of industrial activity in the Arctic regions (Finkel et al., 1986; Li et al., 1993; Li and Barrie, 1993; Colin et al., 1997; Norman et al., 1999; Goto-Azuma and Koerner, 2001; Toom-Sauntry and Barrie, 2002). Other major ion species measured show seasonal trends that are similar to those that have been previously identified for the high-latitude Arctic region (Finkel et al., 1986; Mayewski et al., 1990; Li et al., 1993; Li and Barrie, 1993; Colin et al., 1997; Fischer et al., 1998; Norman et al., 1999; Toom-Sauntry and Barrie, 2002). A small peak in the SO_4^{2-} concentration occurs in July/August at approximately 0.7 m along with corresponding peaks in both nitrate (NO_3^-) and chloride (Cl^-) concentrations. This spike is likely the result of increased anthropogenic inputs as evidenced by the increases in the NO_3^- content in snow which have been shown to occur during the industrial period. Similarly, Cl^- concentrations have also been associated with anthropogenic sources, particularly coal. Moreover, the lighter $\delta^{34}S$ value associated with this spike (+5.6‰) is close to the +3‰ signature of the anthropogenic component, indicating the SO_4^{2-} is likely derived from anthropogenic rather than volcanic sources.

4.3. Anthropogenic and natural S source contributions to sulfate

Distinguishing S sources using only SO_4^{2-} concentration and ion chemistry is difficult at best; but, using S isotope ratios permits seasonal source contributors of S to be broadly identified. The major ion data together with the corrected S isotope data were used in mass balance models to characterize the seasonal S isotopic shifts and to estimate the relative contributions of anthropogenic (fossil fuel burning) and natural (sea salt, dust, and marine biogenic) S sources. The relative contributions of each end-member (Inilchek: anthropogenic and evaporite dust; Summit: anthropogenic + volcanic, dust, marine biogenic, and sea salt) and the estimated contribution of each to the total SO_4^{2-} concentration for the Inilchek samples were determined using a two-component mass balance model and for the Summit samples were determined using a three-component mixing model. These results are shown in Fig. 11a and b (Inilchek) and Fig. 12a and b (Summit). In the models, the measured isotopic composition is apportioned using the following equations:

$$\textbf{Inilchek}: \quad \delta^{34}S_{bc} = f_{nss}\delta_{nss}; \quad f_{nss}\delta_{nss} = f_a\delta_a + f_d\delta_d; \quad f_{nss} = f_a + f_d = 1 \tag{5}$$

$$\textbf{Summit}: \quad \delta^{34}S_{bc} = f_{ss}\delta_{ss} + f_{nss}\delta_{nss}; \quad f_{nss}\delta_{nss} = f_{av}\delta_{av} + f_d\delta_d + f_{mb}\delta_{mb} \tag{6}$$

For the Summit site the fractional contribution (f_{ss}) of sea salt was calculated assuming the mass ratio of SO_4^{2-} to Na^+ (k) is 0.25 in bulk seawater and that this ratio holds for sea salt in ice:

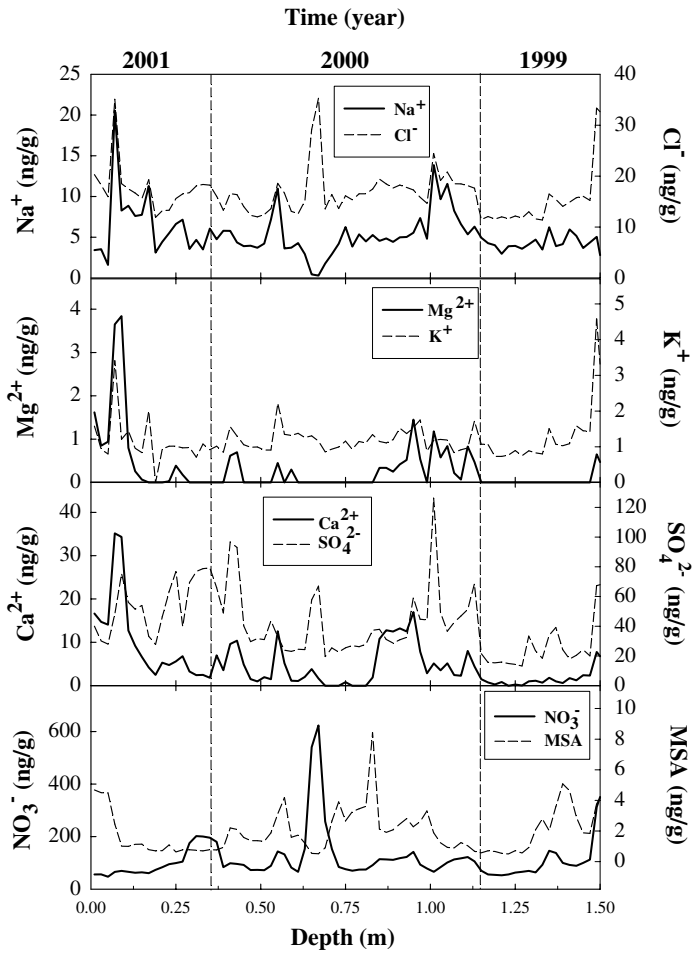

Fig. 10. Concentrations for all soluble major ion species in time (depth) series for the Greenland snow pit. Vertical dashed lines mark the year. All data shown were determined by IC (Uncertainties = ±5%).

$$f_{ss} = \frac{k[Na^+]}{[SO_4{}^{2-}]} \tag{7}$$

The nss$SO_4{}^{2-}$ fraction is $f_{nss} = 1 - f_{ss}$. The nss$SO_4{}^{2-}$ S isotope composition was then derived from $\delta^{34}S_{bc} = f_{ss}\delta_{ss} + (1 - f_{ss})\delta_{nss}$ and is calculated as:

$$\delta_{nss} = \frac{\delta^{34}S_{bc} - f_{ss}\delta_{ss}}{1 - f_{ss}} \tag{8}$$

The dust fraction at Summit was derived from the nss-calcium content assuming the mass ratio for soil and dust emissions is $SO_4{}^{2-}/Ca^{2+} = 0.18$ (Legrand et al., 1997).

The $\delta^{34}S$ values used in the Inilchek model (+20‰ for evaporite dust and 0‰ for anthropogenic) were based on the compositions identified by Kreutz and Sholkovitz (2000) and Pruett et al. (2004a). The $\delta^{34}S$ value used for the anthropogenic component is lighter than the value suggested in previous studies, $\delta^{34}S = +5.4‰$ (Kreutz and Sholkovitz, 2000) and +5‰ (Pruett et al., 2004a) because the predominant fossil fuel sources from surrounding industrial regions have $\delta^{34}S$ values that tend toward lighter values.

The isotopic signatures used in the model for Summit were $\delta_{av} = +3 \pm 1.6‰$ (average of the anthropogenic and non-eruptive volcanic signatures), $\delta_{mb} = +18.6 \pm 0.9‰$, and $\delta_{ss} = +21 \pm 0.2‰$. Anthropogenic and volcanic S are included together as their signatures are indistinguishable. The dust component was determined using the model of Patris et al. (2002) where the isotopic value and the uncertainty are determined assuming the extreme case where the $\delta^{34}S$ value is 20‰ apart from the remaining $\delta^{34}S_{nss}$ ($f_{mb}\delta_{mb} + f_{av}\delta_{av}$). For this study the average contribution from dust was less than 2%.

The isotopic compositions of the end-member sources in some cases are not very well-constrained. This is particularly true for dust being delivered to the Inilchek region. Consequently, the source apportionment results are a coarse estimate until the end-member sources are better characterized. Additionally, error bars are not included because of these large uncertainties.

4.3.1. Inilchek

The mass balance results for the Inilchek show that anthropogenic $SO_4{}^{2-}$ contribution to the $SO_4{}^{2-}$ being deposited dominates during all the seasons representing an average of ≈71% while contributions from evaporite dust were ≈29% (Fig. 11a). The lowest $\delta^{34}S_{bc}$ values

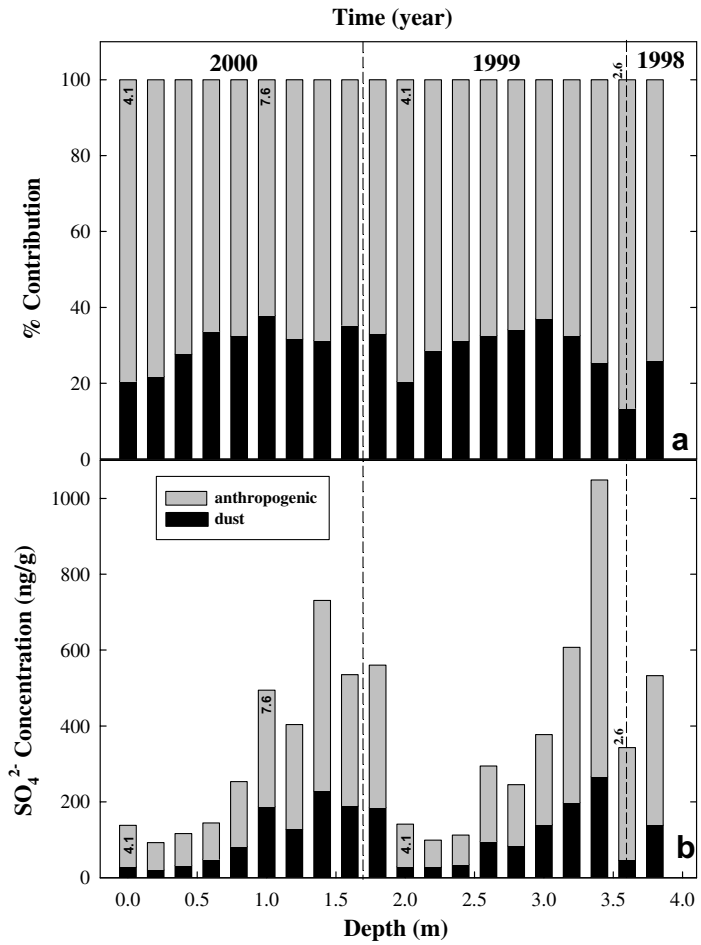

Fig. 11. (a) Relative percent contributions of each sulfate source contributor—anthropogenic and evaporite dust—for the Inilchek site and (b) estimates of the contribution of each to the total sulfate in each snow pit sample.

(+2.6‰ and +4.1‰) observed show a higher anthropogenic input (80–87%) paired with a lower dust input (13–21%). The highest $\delta^{34}S_{bc}$ values (+7.4‰ and +7.6‰) show an increased input of dust (≈37%), up to a factor of almost 3 higher relative to the samples with the lowest $\delta^{34}S$ values, and a reduced input of anthropogenic S (≈63%). Additionally, the $\delta^{34}S$ values appear to increase in the winter months and decrease in the summer months of both years showing an apparent seasonal trend. Deposition of SO_4^{2-} appears to increase in winter/spring of both 1998/1999 (2.5–3.75 m) and again in 1999/2000 (0.7–1.8 m) (Fig. 11b). These increases are associated with an increased input of both S sources. Also, two periods of decreased SO_4^{2-} deposition, summer 2000 (≈0–0.7 m) and summer/fall 1999 (2.0–2.5 m), are represented in the snow pit where a simultaneous reduction in these source contributions occur. During these periods of decreased deposition, anthropogenic S dominates accounting for a larger fraction (≈74%) of total deposition. Anthropogenic inputs also dominate during periods of increased deposition but are slightly smaller (66–71%). Interestingly, although there is a clear seasonal trend in sulfate deposition, the anthropogenic contribution to the total SO_4^{2-} concentration dominates whether or not the overall total SO_4^{2-} deposition is high or low.

In contrast to this study, Pruett et al. (2004a) determined for the 1999 summer season 60% of the SO_4^{2-} being delivered to the Inilchek was from evaporite dust, and 40% was anthropogenic. This result, however, was strongly influenced by a single dust event that contributed 78% of the SO_4^{2-}. In reality the majority of the SO_4^{2-} delivered during the 1999 summer season, which corresponded to a period of lower dust input, was of anthropogenic origin, accounting for nearly 83% of the SO_4^{2-} deposited. Based on our data anthropogenic S contributions during the lower dust periods similarly accounted for 74% of the SO_4^{2-} being deposited with the highest contribution (80–87%) corresponding with lowest $\delta^{34}S_{bc}$ values (+2.6‰ and +4.1‰).

The simultaneous increases and decreases in anthropogenic and evaporite dust SO_4^{2-} deposition suggest that the meteorological conditions and delivery mechanism(s) for these sources to the Inilchek region are similar. The decreased deposition of both sources may be the result of dilution due to increased precipitation. Aizen et al. (2004) noted that maximum precipitation typically occurs during the summer, the same time reductions in SO_4^{2-} deposition are observed, and possibly also in the spring months for this location. Post-depositional effects are unlikely for this region as melt is negligible. The increase in dust SO_4^{2-}

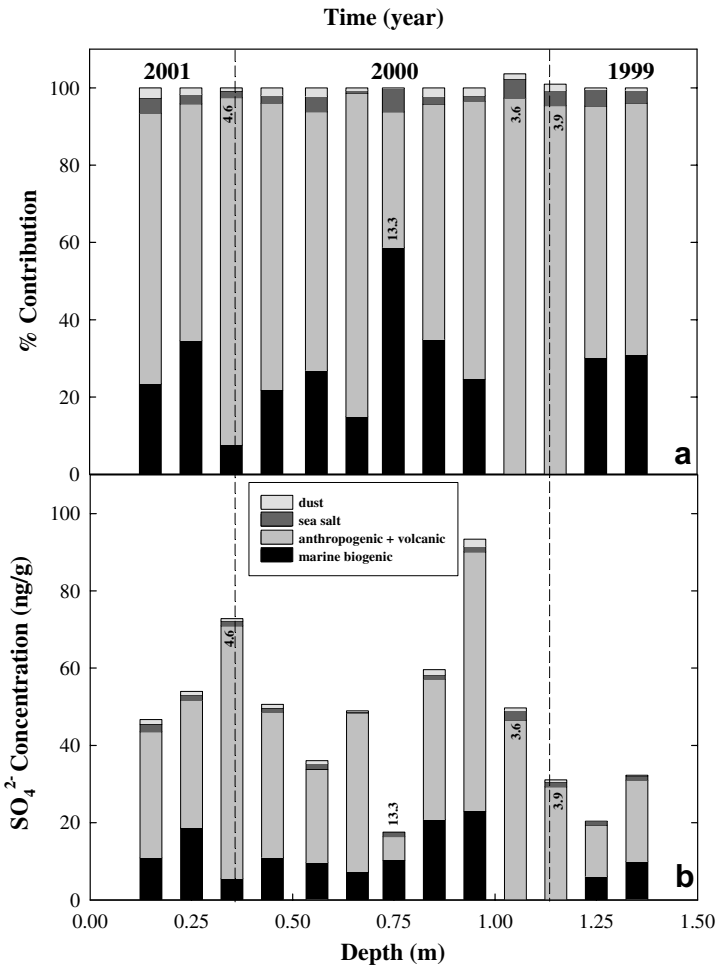

Fig. 12. (a) Relative contributions in percent for each sulfate source contributor—sea salt, anthropogenic, dust, and marine biogenic—for the Greenland snow pit samples and (b) estimated contributions to total sulfate of each source contributor.

deposition observed is likely associated with west to east transport paths that pass over alkali-rich regions. Kreutz and Sholkovitz (2000) suggested west to east transport of aerosols and dust, associated with the Northern Hemisphere jet stream, deliver gypsum dust to the Inilchek, particularly during the summer months. Aizen et al. (2004) observed that during periods of maximum precipitation in the spring and summer months the influx of air masses from the west, which originate over the Atlantic Ocean, Mediterranean, Aral, Caspian and/or Black seas and move along the mid-latitudes at high altitudes, deliver dust derived from the alkali soils (carbonate and gypsum evaporites) of these regions to the Inilchek. Because a simultaneous increase in anthropogenic SO_4^{2-} deposition occurs, it is likely the same west to east air masses may also be responsible for the accompanying increase in anthropogenically derived SO_4^{2-} as they pass over the industrial regions of central Asia. Interestingly, NO_3^- concentrations also increase, which are typically associated with anthropogenic inputs. Aizen et al. (2004) observed that in the winter, spring, and summer months northern and northwestern winds transport anthropogenic aerosols to the Inilchek region from western Kazakhstan and the southern Urals, two highly industrialized regions. It is apparent that the observed increase in both S sources is the result of these synoptic patterns mainly coming from the west. The specific source strength (anthropogenic versus evaporite S) and transport to the Tien Shan is variable and overall deposition of each changes with local and regional atmospheric circulation (Kreutz and Sholkovitz, 2000; Aizen et al., 2004).

The uncertainties in the source $\delta^{34}S$ values for the Inilchek are the largest source of uncertainty in the mass balance estimations. To determine the uncertainty in the calculated relative percent contributions, a sensitivity analysis was performed using the source $\delta^{34}S$ range observed for the end-members in the mass balance equations—evaporite dust (+11‰ to +36‰) and anthropogenic (−5‰ to +5‰). The calculated uncertainty on the relative contributions averages about ±37%. This is much larger than the $\delta^{34}S_{bc}$ measurement uncertainty (0.53%). Because of the large uncertainty on the relative contributions, the results must be interpreted with caution as was previously noted by Pruett et al. (2004a); it is possible that the dust contribution could also dominate. Further optimized sampling for chemical parameters in addition to better characterization of the

isotope composition of the S sources in conjunction with a longer-term high-resolution S isotope record is clearly needed to refine this preliminary assessment.

The seasonality in the $\delta^{34}S$ and SO_4^{2-} deposition records combined with the dominance of anthropogenic sources regardless of the amount of SO_4^{2-} deposited is unique to this study. The snow pit recovered for this work covers approximately 2 years revealing seasonal trends that previously were not known because of poor temporal resolution in earlier snow pit studies. Using the double spike technique the high-resolution $\delta^{34}S$ and SO_4^{2-} deposition records are now accessible and have allowed for a preliminary glimpse into the seasonal trends that exist for this location.

4.3.2. Summit

Similar to the Inilchek samples, the contribution of SO_4^{2-} from anthropogenic sources dominates the Greenland snowpack throughout most of time period represented by the snow pit (mid 1999 to May 2001), with the exception of one point during the summer of 2000 when the marine biogenic contribution to total SO_4^{2-} was larger (Fig. 12a). On average 72% of the nssSO_4^{2-} being contributed to Summit was from anthropogenic sources while 23% was from marine biogenic, and <2% was derived from dust. Sea salt contribution was 3%. These results are similar to the findings of the Li and Barrie (1993) study from Alert, Canada where the marine biogenic contribution was 25–30% during June and August and <14% for the remaining seasons, sea salt was between 1% and 8% year round, and anthropogenic was approximately 62–74% during the summer months but increased during other times of the year. Although conditions are quite different at a high-elevation site like Summit than at sea-level locations the similarity of the mass balance results is remarkable. The lower $\delta^{34}S_{bc}$ values (+3.6‰, +3.9‰, and +4.6‰) that were measured during the winter months in this study show that almost 100% of the nssSO_4^{2-} is from anthropogenic sources with contributions ranging from 90% to 97%. The ^{34}S-enriched $\delta^{34}S_{bc}$ value observed in June/July of 2000 (+13.3‰) is associated with a considerable reduction in anthropogenic input, which resulted in the marine biogenic fraction comprising 58% of the nssSO_4^{2-} and the contribution from anthropogenic sources being reduced to 35%.

Total SO_4^{2-} deposition in winter and spring is typically larger than during the other seasons and corresponds to lighter $\delta^{34}S$ values indicating a larger fraction of the SO_4^{2-} is derived from anthropogenic S (Fig. 12b). The proportion of SO_4^{2-} being contributed from marine biogenic sources is relatively constant through most of the seasons with the exception of the winter months where a substantial decrease in this component can occur as seen in the winter of 1999/2000. Typically, marine biogenic contributions are larger in the spring and summer months associated with spring ice melt and negligible in the fall and winter months (Li and Barrie, 1993; Norman et al., 1999). Sea salt and dust contributions also remain relatively constant throughout the entire year with sea salt contributions not larger than 6.5% and dust not larger than 2.7%.

The observed changes in SO_4^{2-} concentrations, increasing in winter and spring and decreasing in summer and fall, likely occur because of meteorological and source seasonality effects. Specifically, anthropogenic contributions to SO_4^{2-} deposited at Summit are primarily derived from Eurasia where a persistent anticyclone over northern Asia in winter and spring forces some of the air pollution from Europe and Russia to the Arctic region causing increases in SO_4^{2-} deposition (Christensen, 1997) (Fig. 7). Additionally, the scavenging by precipitation is at its lowest during this time of year; therefore, S species do not fall out prior to reaching the Arctic (Davidson et al., 1993; Li and Barrie, 1993). Thus, this pool of S species may undergo photochemical reactions during polar sunrise in spring. These aerosols and gases that are photochemically produced are more readily scavenged by snow allowing for the observed increase in SO_4^{2-} (Finkel et al., 1986). The timing of the peak concentrations corresponds to when anthropogenic contributions increase and become dominant, eliminating SO_4^{2-} from volcanic activity as a contributor. This suggests that background non-eruptive gaseous emissions are presumably the only contributors of SO_4^{2-}. Conversely, the typically lower concentration values in summer occur because northward transport of air masses is weaker and higher precipitation causes S species to fall out prior to reaching the Arctic. Ultimately, the relative contribution of SO_4^{2-} coming into the region from each of these sources is primarily dependent upon the flux of the anthropogenic component. The high-resolution data obtained here is consistent with a seasonal pattern characterized by anthropogenic SO_4^{2-} deposition and shows the large role this source plays in the S cycle for this site.

As with the Inilchek results, a sensitivity analysis was performed using the 1σ uncertainties reported for the input parameters (δ_{av}, δ_d, δ_{mb}) to the mass balance equation, to identify the component contributing the largest portion of uncertainty to the estimates. The uncertainty on the anthropogenic + volcanic composition, +1.6‰, contributed approximately ±14% uncertainty. The uncertainties contributed from the marine biogenic composition (δ_{mb}), with an uncertainty of ±0.9‰, and the dust component (δ_d), with a range of uncertainties from ±0.1‰ to 0.6‰, to the relative contribution calculations was <2% for both. The uncertainty from the $\delta^{34}S_{bc}$ measurement error (including blank uncertainty) is ±5%, which is an order of magnitude larger than the uncertainty from this same component for the Inilchek samples; this is expected because of the larger relative blank contributions in these samples. Although better characterization of the end member isotope composition of the anthropogenic fraction would reduce uncertainty, the sensitivity analysis here shows that the conclusions drawn about the Summit site are robust relative to the possible variations in the end member compositions, unlike that for the Inilchek samples.

5. SUMMARY AND CONCLUSIONS

The $\delta^{34}S$ and SO_4^{2-} concentration measurements demonstrate the double spike MC-TIMS technique is a credible and perhaps a superior method for analysis of μg/L levels of SO_4^{2-} in natural samples. In both study sites the calculated precisions were achieved using less meltwater and

on smaller sample sizes, than are typically used for gas source analysis and are comparable to or better than the precisions obtained by these techniques for larger sample sizes (typically ±1‰). The new method also offers two additional advantages. First, because it uses an internal standard rather than an external standard it is intrinsically accurate, insofar as only isotope ratios need to be measured; therefore, complete recovery of the sample is not required for unbiased results. Also, loses during drying and/or chemical reduction of the sample that may cause mass fractionation are accounted for by adding the spike prior to sample processing. This is a considerable advantage for small sample sizes (<1 μmol S) where losses can result in potentially large biases without the use of an internal standard. Second, it provides a better evaluation of both the blank amount and its composition. The blank problem exists no matter what measurement technique is employed for S isotope analysis. The measurements made here demonstrate not only that blanks must be measured to assess the accuracy of the $\delta^{34}S$ data but also better control of blanks could enable attainment of 0.1‰ precision for even the smallest samples.

The $\delta^{34}S$ and SO_4^{2-} concentration results also demonstrate not only the capability of the new technique to measure the small (ng/g) sample amounts thus allowing access to the high-resolution $\delta^{34}S$ record contained in snow, but also highlight the potential for identifying the seasonal SO_4^{2-} sources contributing to high-elevation precipitation with improved source $\delta^{34}S$ characterization. The data obtained show that the main SO_4^{2-} contributors to the Inilchek are anthropogenic and evaporite dust, while SO_4^{2-} being delivered to Summit is mostly anthropogenic and marine biogenic in origin. Overall, the results show that anthropogenic inputs tend to dominate, averaging almost 72%, for both sites. The data specifically show an apparent seasonality for both the Inilchek and Summit, where values are typically ^{34}S-enriched in the spring and/or summer months and ^{34}S-depleted in the winter months for both sites. The ^{34}S-enriched summer values for the Inilchek site correspond to a decrease in both the anthropogenic and dust inputs, but anthropogenic deposition accounts for a larger proportion of the SO_4^{2-} deposition. Similarly, in winter anthropogenic deposition also accounts for a larger proportion of the SO_4^{2-} deposition, but in this case an increase in the deposition of both components occurs. The ^{34}S-depleted winter values for the Summit site are attributed to larger anthropogenic contribution while the ^{34}S-enriched summer value is attributed to a considerable reduction of this same component.

At both site locations, total SO_4^{2-} concentrations show considerable variability. Peaks in SO_4^{2-} concentration in the Inilchek snow pit occur in the winter/spring months while reduced deposition of SO_4^{2-} occurs in summer and fall. The mechanism responsible for the increased deposition in winter/spring is likely caused by increased transport of air masses from west to east. In the Summit snow pit, peaks in SO_4^{2-} concentration occur in winter and early spring. This enhancement is likely caused by changing meteorological conditions and source seasonality effects in combination with increased transport of air pollution from the mid-latitudes and decreased scavenging by precipitation at this time of year (Finkel et al., 1986; Davidson et al., 1993; Li and Barrie, 1993). Overall, the deposition of anthropogenic and evaporite dust SO_4^{2-} to the Inilchek site are quite variable but seasonally consistent. For the Summit site sea salt and dust SO_4^{2-} source contributions are relatively constant throughout the year. Marine biogenic SO_4^{2-} inputs are also relatively constant through the year with only periodic reductions in the winter months. Consequently, it appears that the variability in the S deposition is dominated by changes in the anthropogenic contribution. This again demonstrates the importance of understanding the timing and magnitude of the anthropogenic input and the large role this S source plays in the S cycle for the Summit site.

DISCLAIMER

Certain commercial equipment, instruments or materials are identified in this work to specify adequately the experimental procedure. Such identification does not imply recommendation or endorsement by the National Institute of Standards and Technology, nor does it imply that the materials or equipment identified are necessarily the best available for this purpose.

ACKNOWLEDGMENTS

Financial support for this study from the EPA Star Fellowship program (#U915356) to J.L.M. and from the National Aeronautics and Space Administration (NASA) (51-622-83-72WBS) and the National Science Foundation (NSF) to Dr. Christopher A. Shuman is gratefully acknowledged. Sample collection from the Inilchek Glacier was supported by NSF ATM Grant 0000560 to Dr. Karl J. Kreutz. The authors also thank Dr. Richard J. Walker, Director of the Isotope Geochemistry Laboratory in the Department of Geology at the University of Maryland for use of the VG multiple-collector mass spectrometer (VG Sector 54) for this work, and Douglas Introne and Sharon Sneed of the University of Maine Climate Change Institute for stable isotope and major ion analyses. Finally, we thank all reviewers for their critical analysis and many helpful comments. Special thanks are extended to Dr. Alan J. Kaufman for additional editing of the manuscript at the author's request.

APPENDIX A. SUPPLEMENTARY DATA

Supplementary data associated with this article can be found, in the online version, at doi:10.1016/j.gca.2008.05.036.

REFERENCES

Aizen V. B., Aizen E., Melack J. and Martma T. (1996) Isotopic measurements of precipitation on central Asian glaciers (southeast Tibet, northern Himalayas, central Tien Shan). *J. Geophys. Res.* **101**, 9185–9196.

Aizen V. B., Aizen E. M., Dozier J., Melack J. M., Sexton D. D. and Nesterov N. (1997) Glacial regime of the highest Tien Shan mountain, Pobeda-Khan Tengry massif. *J. Glaciol.* **145**, 503–512.

Aizen V. B., Aizen E. M., Melack J. M., Kreutz K. J. and Cecil L. D. (2004) Association between atmospheric circulation patterns and firn-ice core records from the Inilchek glacierized area, central Tien Shan, Asia. *J. Geophys. Res.* **109**. doi:10.1029/2003JD003894.

Alley R. B. and Anandarkrishnan S. (1995) Variations in melt-layer frequency in the GISP2 ice core: implications for Holocene summer temperatures in central Greenland. *Ann. Glaciol.* **21**, 64–70.

Barth M., Rasch P. J., Kiehl J. T., Benkovitz C. M. and Schwartz S. E. (2000) Sulfur chemistry in the National Center for Atmospheric Research Community Climate Model: description, evaluation, features and sensitivity to aqueous chemistry. *J. Geophys. Res.* **105**, 1387–1415.

Biscaye E., Grousset F. E., Revel M., Van der Gaast S., Zielinski G. A., Vaars A. and Kulka G. (1997) Asian provenance of glacial dust (stage 2) in the Greenland Ice Sheet Project 2 Ice Core, Summit, Greenland. *J. Geophys. Res.* **102**, 26765–26781.

Bory A. J. M., Biscaye P. E., Svensson A. and Groussett F. E. (2002) Seasonal variability in the origin of recent atmospheric mineral dust at North GRIP, Greenland. *Earth Planet. Sci. Lett.* **196**, 123–134.

Bory A. J. M., Biscaye P. E. and Groussett F. E. (2003a) Two distinct seasonal Asian source regions for mineral dust deposited in Greenland (NorthGRIP). *Geophys. Res. Lett.* **30**, 16-1–16-4.

Bory A. J. M., Biscaye P. E., Piotrowski A. M. and Steffensen J. P. (2003b) Regional variability of ice core dust composition and provenance in Greenland. *Geochem. Geophys. Geosyst.*. Art. No. 1107.

Brimblecombe P., Hammer C., Rodhe H., Ryaboshapko A. and Boutron C. F. (1989) Human influence on the sulphur cycle. In *Evolution of the Global Biogeochemical Sulphur Cycle, SCOPE 39* (eds. P. Brimblecombe and A. Y. Lein). Wiley, Chichester, pp. 77–121.

Calhoun J. A., Bates T. S. and Charlson R. J. (1991) Sulfur isotope measurements of submicrometer sulfate aerosol particles over the Pacific Ocean. *Geophys. Res. Lett.* **18**, 1877–1880.

Chin M., Rood R. B., Lin S.-J., Muller J.-F. and Thompson A. M. (2000a) Atmospheric sulfur cycle simulated in the Global Model GOCART: model description and global properties. *J. Geophys. Res.* **105**, 24671–24687.

Chin M., Savoie D. L., Huebert B. J., Bandy A. R., Thornton D. C., Bates T. S., Quinn P. K., Saltzman E. S. and De Bruyn W. J. (2000b) Atmospheric sulfur cycle simulated in the Global Model GOCART: comparison with field observations and regional budgets. *J. Geophys. Res.* **105**, 24689–24712.

Christensen J. H. (1997) The Danish Eulerian Hemispheric Model—a three-dimensional air pollution model used for the Arctic. *Atmos. Environ.* **31**, 4169–4191.

Claquin T., Schulz M. and Balkanski Y. J. (1999) Modeling the mineralogy of atmospheric dust sources. *J. Geophys. Res.* **104**, 22243–22256.

Claypool G. E., Holser W. T., Kaplan I. R., Sakai H. and Zak I. (1980) The age curves of sulfur and oxygen isotopes in marine sulfate and their mutual interpretation. *Chem. Geol.* **28**, 199–260.

Colin J. L., Lim B., Herms E., Genet F., Drab E., Jafferzo J. L. and Davidson C. I. (1997) Air to snow mineral transfer—crustal elements in aerosols, fresh snow and snow pits on the Greenland ice sheet. *Atmos. Environ.* **31**, 3395–3406.

Cortecci G. and Longinelli A. (1970) Isotopic composition of sulfate in rain water, Pisa, Italy. *Earth Planet. Sci. Lett.* **8**, 36–40.

Davidson C. I., Jaffrezo J.-L., Small M. J., Summers P. W., Olson M. P. and Borys R. D. (1993) Trajectory analysis of source regions influencing the South Greenland Ice Sheet during the Dye 3 gas and aerosol sampling program. *Atmos. Environ.* **27A**, 2739–2749.

Dignon J. and Hameed S. (1989) Global emissions of nitrogen and sulfur oxides from 1860–1980. *J. Air Pollut. Control Assoc.* **3**, 180–186.

Ding T., Valkiers S., Kipphardt H., De Bievre P., Taylor P. D. P., Gonfiantini R. and Krouse R. (2001) Calibrated sulfur isotope abundance ratios of three IAEA sulfur isotope reference materials and V-CDT with a reassessment of the atomic weight of sulfur. *Geochim. Cosmochim. Acta* **65**, 2433–2437.

Epstein S. and Mayeda T. (1953) Variation of ^{18}O content from natural sources. *Geochim. Cosmochim. Acta* **4**, 213–244.

Eugster O., Tera F. and Wasserburg G. J. (1969) Isotopic analysis of barium in meteorites and in terrestrial samples. *J. Geophys. Res.* **74**, 3897–3908.

Finkel R. C., Langway, Jr., C. C. and Clausen H. B. (1986) Changes in precipitation chemistry at Dye 3, Greenland. *J. Geophys. Res.* **91**, 9849–9855.

Fischer H., Wagenbach D. and Kipfstuhl J. (1998) Sulfate and nitrate firn concentrations on the Greenland ice sheet 1. Large-scale geographical deposition changes. *J. Geophys. Res.* **103**, 21927–21934.

Fisher D. A., Reeh N. and Clausen H. B. (1985) Stratigraphic noise in time series derived from ice cores. *Ann. Glaciol.* **14**, 65–71.

Fisher D. A., Koerner R. M., Kuivinen K., Clausen H. B., Johnsen S. J., Steffense J.-P. and Gunderstrup N. (1996) Inter-comparison of ice core $\delta^{18}O$ and precipitation records from sites in Canada and Greenland over the last 3,500 years and over the last few centuries in detail using EOF techniques. In *Climate Variations and Forcing Mechanisms of the Last 2000 Years* (eds. R. S. Bradley, J. Jouzel and P. D. Jones). Springer-Verlag, New York, pp. 297–330.

Goto-Azuma K. and Koerner R. M. (2001) Ice core studies of anthropogenic sulfate and nitrate trends in the Arctic. *J. Geophys. Res.* **106**, 4959–4969.

Green J. R., Cecil L. D., Synal H. A., Santos J., Kreutz K. J. and Wake C. P. (2004) A high-resolution record of chlorine-36 nuclear-weapons-tests fallout from Central Asia. *Nucl. Instrum. Meth.* **223**, 854–857.

Hayes J. M. (2002) Practice and principles of isotopic measurements in organic geochemistry. In *Organic Geochemistry of Contemporaneous and Ancient Sediments (1983). Published by the Great Lakes Section of the Society of Economic Paleontologists and Mineralogist* (ed. W. G. Meinschein, Reedited by Alex L. Sessions), pp. 1–25. Available from: <http://www.gps.caltech.edu/classes/ge148c/Practice%20and%20Principles.pdf>.

Herut B., Spiro B., Starinsky A. and Katz A. (1995) Sources of sulfur in rainwater as indicated by isotopic $\delta^{34}S$ data and chemical composition, Israel. *Atmos. Environ.* **29**, 851–857.

Holmden C., Eglington B. A. and Papanastassiou D. A. (2005a) High mass resolution plasma mass spectrometry of Cr isotopes. In *14thAnnual Goldschmidt Conference*, Moscow, Idaho, 2005; CD-ROM, A552 (abstr.).

Holmden C. (2005b) Measurement of $\delta^{44}Ca$ using a ^{43}Ca–^{42}Ca double-spike TIMS technique. Saskatchewan Geological Survey. *Summ. Investig.* **1**, 1–7.

IPCC (Intergovernmental Panel on Climate Change) (2001) Third Assessment Report—Climate Change 2001 (eds. J. T. Houghton et al.). Cambridge University Press, New York.

Johnsen S. J., Clausen H. B., Dansgaard W., Fuhrer K., Gundestrup N., Hammer C. U., Iversen P., Jouzel J., Stauffer B. and Steffensen J. P. (1992) Irregular glacial interstadials recorded in a new Greenland ice core. *Nature* **359**, 311–313.

Johnson T. M., Herbel M. J., Bullen T. D. and Zawislanski P. T. (1999) Selenium isotope ratios as indicators of selenium sources and oxyanion reduction. *Geochim. Cosmochim. Acta* **63**, 2775–2783.

Kang S., Mayewski P. A., Qin D., Yan Y., Hou Y., Zhang D. and Kreutz K. J. (2002) Glaciochemical records from a Mt. Everest ice core: relationship to atmospheric circulation over Asia. *Atmos. Environ.* **36**, 3351–3361.

Koch D., Jacob D., Tegen I., Rind D. and Chin M. (1999) Tropospheric sulfur simulation and sulfate direct radiative forcing in the GISS GCM. *J. Geophys. Res.* **104**, 23799–23823.

Kreutz K. J. and Sholkovitz E. R. (2000) Major element, rarer earth element, and sulfur isotopic composition of a high-elevation firn core: sources and transport of mineral dust in central Asia. *Geochem. Geophys. Geosyst.* **1**, paper number 2000GC000082.

Kreutz K. J., Aizen V. B., Cecil L. D. and Wake C. P. (2001) Oxygen isotopic and soluble ionic composition of precipitation recorded in a shallow firn core, Inilchek Glacier (Central Tien Shan). *J. Glaciol.* **47**, 548–554.

Kreutz, K.J., Wake, C.P., Aizen, V.B., Cecil, L.D., Synal, H.-A. (2003) Seasonal deuterium excess in a Tien Shan ice core: influence of moisture transport and recycling in Central Asia. *Geophys. Res. Lett.* **30**, Art. No. 1922.

Krouse, H.R., Grinenko, V.A. (1991) *Stable Isotopes: Natural and Anthropogenic Sulphur in the Environment*, Vol. 43. John Wiley & Sons, New York.

Lefohn A. S., Husar J. D. and Husar R. B. (1999) Estimating historical anthropogenic global sulfur emission patterns for the period 1850–1990. *Atmos. Environ.* **33**, 3435–3444.

Legrand M. and Mayewski P. A. (1997) Glaciochemistry of polar ice cores: a review. *Rev. Geophys.* **35**, 219–243.

Legrand M., Hammer C., De Angelis M., Savarino J., Delmas R., Clausen H. and Johnsen S. J. (1997) Sulfur-containing species (methanesulfonate and SO_4) over the last climatic cycle in the Greenland Ice Core Project (central Greenland) ice core. *J. Geophys. Res.* **102**, 26663–26679.

Li S.-M., Barrie L. A. and Sirois A. (1993) Biogenic sulfur aerosol in the Arctic troposphere: 2. Trends and seasonal variations. *J. Geophys. Res.* **98**, 20623–20631.

Li S.-M. and Barrie L. A. (1993) Biogenic sulfur aerosol in the Arctic troposphere: 1. Contributions to total sulfate. *J. Geophys. Res.* **98**, 20613–20622.

Mann J. L. (2005) Determination of Sulfur Isotope Composition in Sulfate from Two High Elevation Snow pits by Multi-Collector Thermal Ionization Mass Spectrometry Using a Double Spike. Ph.D. Thesis, University of Maryland.

Mann J. L. and Kelly W. R. (2005) Measurement of sulfur isotope composition ($\delta^{34}S$) by multiple-collector thermal ionization mass spectrometry using a ^{33}S–^{36}S double spike. *Rapid Commun. Mass Spectrom.* **19**, 3429–3441.

Mayewski P. A., Lyons W. B., Spencer M. J., Twickler M. S., Dansgaard W., Koci B., Davidson C. I. and Honrath R. E. (1986) Sulfate and nitrate concentrations from a South Greenland Ice Core. *Science* **232**, 975–977.

Mayewski P. A., Lyons W. B., Spencer M. J., Twickler M. S., Buck C. F. and Whitlow S. (1990) An ice core record of atmospheric response to anthropogenic sulphate and nitrate. *Nature* **346**, 554–556.

McArdle N. C. and Liss P. S. (1995) Isotopes and atmospheric sulfur. *Atmos. Environ.* **29**, 2553–2556.

McArdle N. C., Liss P. S. and Dennis P. (1998) An isotopic study of atmospheric sulphur at three sites in Wales and at Mace Head, Eire. *J. Geophys. Res.* **103**, 31079–31094.

Morrison J., Brockwell T., Merren T., Fourel F. and Phillips A. M. (2001) On-line high-precision stable hydrogen isotopic analyses on nanoliter water samples. *Anal. Chem.* **73**, 3570–3575.

Mukai H., Tanaka A., Fujii T., Zeng Y. Q., Hong Y. T., Tang J., Guo S., Xue H. S., Sun Z. L., Zhou J. T., Xue D. M., Zhao J., Zhai G. H., Gu J. L. and Zhai P. Y. (2001) Regional characteristics of sulfur and lead isotope ratios in the atmosphere at several Chinese urban sites. *Environ. Sci. Technol.* **35**, 1064–1071.

Neftel A., Beer J., Oeschger H., Zurcher F. and Finkel R. C. (1985) Sulphate and nitrate concentrations in snow from South Greenland 1895–1978. *Nature* **314**, 611–613.

Nielsen H. (1974) Isotopic composition of the major contributors to atmospheric sulfur. *Tellus* **26**, 213–221.

Nielsen H., Pilot J., Grinenko L. N., Grinenko V. A., Lein A. Y., Smith J. W. and Pankina R. G. (1991) Lithospheric sources of sulphur. In *Stable Isotopes: Natural and Anthropogenic Sulphur in the Environment* (eds. H. R. Krouse and V. A. Grinenko). John Wiley & Sons, pp. 133–176.

Newman L., Krouse H. R. and Grinenko V. A. (1991) Sulphur isotope variations in the atmosphere. In *Stable Isotopes: Natural and Anthropogenic Sulphur in the Environment* (eds. H. R. Krouse and V. A. Grinenko). John Wiley & Sons, p. 440.

Norman A. L., Barrie L. A., Toom-Sauntry D., Sirois A., Krouse H. R., Li S. M. and Sharma S. (1999) Sources of aerosol sulphate at Alert: apportionment using stable isotopes. *J. Geophys. Res.* **104**, 11619–11631.

Nriagu J. O., Holdway D. A. and Coker R. D. (1987) Biogenic sulfur and the acidity of rainfall in remote areas of Canada. *Science* **237**, 1189–1192.

Nriagu J. O., Coker R. D. and Barrie L. A. (1991) Origin of sulphur in Canadian Arctic Haze from isotope measurements. *Nature* **349**, 142–145.

Ohizumi T., Fukuzaki N. and Kusakabe M. (1997) Sulfur isotope view on the sources of sulfur in atmospheric fallout along the coast of the Sea of Japan. *Atmos. Environ.* **31**, 1339–1348.

Patris N., Delmas R. J. and Jouzel J. (2000a) Isotopic signatures of sulfur in shallow Antarctic ice cores. *J. Geophys. Res.* **105**, 7071–7078.

Patris N., Mihalopoulos N., Baboukas E. D. and Jouzel J. (2000b) Isotopic composition of sulfur in size-resolved marine aerosols above the Atlantic Ocean. *J. Geophys. Res.* **105**, 14449–14457.

Patris N., Delmas R. J., Legrand M., De Angelis M., Ferron F. A., Stievenard M. and Jouzel J. (2002) First sulfur isotope measurements in central Greenland ice cores along the preindustrial and industrial periods. *J. Geophys. Res.* **107**, ACH 6-1–ACH 6-13.

Paulsen P. J. and Kelly W. R. (1984) Determination of sulfur as arsenic monosulfide by Isotope Dilution Thermal Mass Spectrometry. *Anal. Chem.* **56**, 708–713.

Pichlmayer F., Schoner W., Seibert P. and Stichler W. (1998) Stable isotope analysis for characterization of pollutants at high elevation alpine sites. *Atmos. Environ.* **32**, 4075–4085.

Polian G., Lambert G., Ardouin B. and Jegou A. (1986) Long-range transport of continental radon in aubantarctic and Antarctic areas. *Tellus* **38**, 178–189.

Pruett L. E., Kreutz K. J., Wadleigh M. and Aizen V. (2004a) Assessment of sulfate sources in high-elevation asian precipitation using stable sulfur isotopes. *Environ. Sci. Technol.* **38**, 4728–4733.

Pruett L. E., Kreutz K. J., Wadleigh M., Mayewski P. A. and Kurbatov A. (2004b) Sulfur isotopic measurements from a West Antarctic ice core: implications for sulfate source and transport. *Ann. Glaciol.* **39**, 161–168.

Querol X., Alastucy A., Chaves A., Spiro B., Plana F. and Lopez-Soler A. (2000) Sources of natural and anthropogenic sulphur around the Teruel power station, NE Spain: inferences from sulphur isotope geochemistry. *Atmos. Environ.* **34**, 333–345.

Rasch P. J., Barth M. C., Kiehl J. T., Schwartz S. E. and Benkovitz C. M. (2000) A description of the global sulfur cycle and its

controlling processes in the National Center for Atmospheric Research Community Climate Model, Version 3. *J. Geophys. Res.* **105**, 1367–1385.

Rees C. E., Jenkins W. J. and Monster J. (1978) The isotopic composition of ocean water sulfate. *Geochim. Cosmochim. Acta* **42**, 377–381.

Russell W. A., Papanastassiou D. A. and Tombrello T. A. (1978) Ca isotope fractionation on the Earth and other solar system materials. *Geochim. Cosmochim. Acta* **42**, 1075–1090.

Saltzman E. S., Brass G. W. and Price D. A. (1983) The mechanism of sulfate aerosol formation: chemical and sulfur isotopic evidence. *Geophys. Res. Lett.* **10**, 513–516.

Shuman C. A., Alley R. B., Anandakrishnan S., White J. W. C., Grootes P. M. and Stearn C. R. (1995) Temperature and accumulation at the Greenland Summit: comparison of high-resolution isotope profiles and satellite passive microwave brightness temperature trends. *J. Geophys. Res.* **100**, 9165–9177.

Shuman C. A., Alley R. B., Fahnestock M. A., Bindschadler R. A., White J. W. C., Winterle J. and McConnell J. R. (1998) Temperature history and accumulation timing for the snow-pack at GISP2, central Greenland. *J. Glaciol.* **44**, 21–30.

Spiro P. A., Jacob D. J. and Logan J. A. (1992) Global inventory of sulfur emissions with $1° \times 1°$ resolution. *J. Geophys. Res.* **97**, 6023–6036.

Taylor B. E., Ding T., Halas S., Breas O. and Robinson B. W. (2000) Accurate Calibration of the V-CDT Scale: Proposed $\delta^{34}S$ values for Calibration and Reference Materials and Methods of Correction for SO_2-based Analyses. *Report of Sulfur Isotope Working Group 8th Advisory Group Meeting on Future Trends in Stable Isotope Reference Materials and Laboratory Quality Assurance*, September 18–22, 2000, IAEA Headquarters, Vienna, Australia.

Todt W., Cliff R. A., Hanser A. and Hoffmann A. W. (1996). In *Earth Processes: Reading the Isotopic Code—Geophysical Monograph 95*. American Geophysical Union, Washington, pp. 159–174.

Toom-Sauntry D. and Barrie L. A. (2002) Chemical composition of snowfall in the High Arctic: 1990–1994. *Atmos. Environ.* **36**, 2683–2693.

Vaughn B. H., White J. W. C., Delmotte M., Trolier M., Cattani O. and Stievenard M. (1998) An automated system for hydrogen isotope analysis of water. *Chem. Geol.* **152**, 309–319.

Wadleigh M. A., Schwarcz H. P. and Kramer J. R. (1996) Isotopic evidence for the origin of sulphate in coastal rain. *Tellus Ser. B* **48**, 44–59.

Wake C. P., Mayewski P. A. and Spencer M. J. (1990) A review of central Asian glaciochemical data. *Ann. Glaciol.* **14**, 301–306.

Wake C. P., Mayewski P. A., Ping W., Yang Q., Jiankang H. and Zichu X. (1992) Anthropogenic sulfate and Asian dust signals in snow from Tien Shan, northwest China. *Ann. Glaciol.* **16**, 45–52.

Wake C. P., Mayewski P. A., Li Z., Han J. and Qin D. (1994) Modern eolian dust deposition in central Asia. *Tellus* **46B**, 220–233.

Wasiuta V., Norman A.-L. and Marshall S. (2006) Spatial patterns and seasonal variation of snowpack sulphate isotopes of the Prince of Wales Icefield, Ellesmere Island, Canada. *Ann. Glaciol.* **43**, 390–396.

Wedepohl, K.H. (1978) *Handbook of Geochemistry* Vol. II. Springer-Verlag, Heidelberg.

White J. W. C., Barlow L. K., Fisher D., Grootes P., Jouzel J., Johnsen S. J., Stuiver M. and Clausen H. (1997) The climate signal in the stable isotopes of snow from Summit, Greenland: results of comparisons with modern climate observations. *J. Geophys. Res.* **102**, 26425–26439.

Associate editor: Clark M. Johnson

Electronic Annex Table A1. $\delta^{18}O$ and δD values used for dating the Inilchek Snow pit.

Depth (m)	$\delta^{18}O$[a]	δD[b]	Depth (m)	$\delta^{18}O$[a]	δD[b]
0	N/A	-97.8	2.05	-10.75	-60.1
0.05	N/A	-98.3	2.10	-9.56	-55.2
0.10	N/A	-39.6	2.15	-10.41	-61.0
0.15	N/A	-38.6	2.20	-11.20	-67.2
0.20	N/A	-61.8	2.25	-11.27	-67.8
0.25	N/A	-58.1	2.30	-11.47	-69.6
0.35	N/A	-48.4	2.35	-12.91	-82.3
0.40	N/A	-33.8	2.40	-12.84	-80.9
0.45	N/A	-50.0	2.45	-12.95	-83.9
0.50	N/A	-89.2	2.50	-13.40	-84.4
0.55	N/A	-75.9	2.55	-13.23	-80.7
0.60	N/A	-59.8	2.60	-12.55	-76.6
0.65	N/A	-59.4	2.65	-11.48	-62.5
0.70	N/A	-67.4	2.70	-12.13	-69.8
0.75	N/A	-42.5	2.75	-14.35	-87.9
0.80	N/A	-58.8	2.80	-14.32	-89.4
0.85	N/A	-55.4	2.85	-15.99	-104.5
0.90	N/A	-43.1	2.90	-16.46	-108.0
0.95	N/A	-29.6	2.95	-15.95	-102.4
1.00	N/A	-34.2	3.00	-17.24	-114.8
1.05	-8.73	-39.4	3.05	-16.36	-104.8
1.10	-9.69	-47.8	3.10	-25.11	-179.1
1.15	-10.13	-52.4	3.15	-15.18	-81.9
1.20	-11.24	-62.3	3.20	-14.58	-92.6
1.25	-11.89	-69.4	3.25	-15.31	-95.5
1.30	-12.26	-71.3	3.30	-16.51	-104.0
1.35	-14.67	-93.9	3.35	-18.16	-121.6
1.40	-15.26	-96.8	3.40	-20.91	-144.0
1.45	-15.24	-95.8	3.45	-24.80	-179.2
1.50	-15.77	-97.1	3.50	-25.72	-186.9
1.55	-17.44	-112.8	3.55	N/A	-147.9
1.60	-20.73	-145.5	3.60	-25.27	-178.7
1.65	-26.26	-189.9	3.65	-27.13	-199.9
1.70	-27.10	-199.0	3.70	-25.29	-177.3
1.75	-26.34	-190.6	3.75	-21.65	-142.4
1.80	-21.33	-144.8	3.80	-19.49	-124.7
1.85	-17.18	-111.6	3.85	-17.63	-95.8
1.90	-16.16	-104.8	3.90	-16.50	-100.9
1.95	-15.20	-96.2	3.95	-16.28	-98.7
2.00	-13.62	-82.8	4.00	-15.44	-99.7

O and D delta values are reported in ‰ relative to VSMOW.

(a) Uncertainty is 0.05‰ (1σ). (b) Uncertainty is 0.5‰ (1σ).

Electronic Annex Table A2. δD values used for dating the Summit Snow pit.

Depth (m)	δD[a]	Depth (m)	δD[a]
0.03	-278.8	0.90	-243.3
0.06	-256.9	0.93	-249.8
0.09	-224.8	0.96	-250.8
0.12	-222.9	0.99	-257.9
0.15	-245.2	1.02	-272.0
0.18	-256.2	1.05	-283.7
0.21	-261.9	1.08	-280.8
0.24	-279.4	1.11	-261.3
0.27	-291.9	1.14	-247.4
0.30	-291.5	1.17	-247.3
0.33	-302.3	1.20	-258.1
0.36	-318.7	1.23	-279.5
0.39	-318.6	1.26	-294.5
0.42	-310.0	1.29	-290.9
0.45	-305.8	1.32	-278.8
0.48	-278.6	1.35	-270.7
0.51	-237.9	1.38	-269.1
0.54	-235.5	1.41	-267.0
0.57	-243.0	1.44	-254.1
0.60	-238.0	1.47	-233.8
0.63	-235.8	1.50	-217.2
0.66	-220.8	1.53	-213.6
0.69	-187.2	1.56	-228.5
0.72	-175.6	1.59	-249.7
0.75	-202.9	1.62	-266.2
0.78	-225.5	1.65	-277.9
0.81	-227.9	1.68	-288.1
0.84	-227.9	1.71	-293.7
0.87	-233.7	1.74	-291.9

D delta values are reported in ‰ relative to VSMOW.

(a) Uncertainty is 0.3‰ (1σ).